Final Report

N01-DC-9-2106

Effects of Remaining Hair Cells on Cochlear Implant Function

P.J. Abbas, C.A. Miller, J.T. Rubinstein, B.K. Robinson, N. Hu,
Hiroyuki Mino, B.A. Abkes, J. Nichols

Department of Otolaryngology - Head and Neck Surgery
Department of Speech Pathology and Audiology
Department of Physiology and Biophysics
University of Iowa
Iowa City, IA 52242

July 31, 2002

Contents

1 Introduction

1.1 Overview

This document summarizes work performed under Contract N01-DC-9-2106. Much of the work has been previously described in the Quarterly Progress Reports which are available at the Neural Prosthesis Program website:

http://npp.ninds.nih.gov/

and at our website:

http://earpower.oto.uiowa.edu/npp/npp.html

While the findings from those reports are summarized in this Final Report, we also make reference to specific progress reports in the text for those wishing more detailed accounts of specific experiments.

In this contract, we have conducted physiological and computational model experiments to assess the effects that functional hair cells have on the mammalian auditory nerve's response to electrical stimulation. This work is relevant to the widening pool of cochlear implant candidates, as audiological criteria (e.g., pure-tone thresholds) are becoming more relaxed and patients with residual hearing are being implanted. Intact hair cells may influence the electrically transduced signal in several ways:

- Acoustically evoked neural activity may interact or compete with electrically evoked activity.
- The very presence of hair cells - without any exogenous acoustic stimuli- may modify the electrically evoked neural response. In this case, electrical stimuli may depolarize hair cells and initiate the release of neurotransmitter resulting in activation of nerve fibers.
- Furthermore, the quiescent release of neurotransmitter - which results in spontaneous neural activity – may modulate the response characteristics of electrically stimulated nerve fibers

To differentiate among these different types of interactions, we often make reference to "direct-nerve" and "hair-cell mediated" modes of response to electrical stimulation. We use the first term to refer to the depolarization of the nerve-fiber membrane by an exogenous electrical field, i.e., the mechanism operative in the electrically stimulated, deaf cochlea. In contrast,

we use the second term to denote a response to an electrical stimulus that involves a functional hair cell. By these definitions, a manifestation of "direct nerve" electrical stimulation is Moxon's short-latency "alpha" response that is elicited by a current pulse (Moxon, 1971). Auditory nerve responses with longer latencies (typically $>$ 1 ms), such as the "delta" and "beta" responses, presumably involve viable hair cells and driven synaptic activity.

1.2 General goals and approach

The experiments of this contract were designed to acquire evoked potentials from the auditory nerve of experimental animal preparations with functional and nonfunctional hair cells. Comparisons of responses from these two preparations were then performed to assess the effect of functional hair cells on the transduction of electrical stimuli delivered by intracochlear electrodes.

If cochlear implant patients with residual hearing can maintain significant hair cell integrity, it is important to define the extent to which direct-nerve and hair-cell mediated responses can be manipulated so as to provide maximum benefit to implanted patients. One important issue is to determine the extent to which individuals may be able to centrally integrate the neural activity generated by hair-cell mediated and direct-nerve electric activation,and the neural activity generated by acoustic transduction. This is best approached by examining the psychophysical performance in human subjects. In this work, however, we have examined direct-nerve and hair-cell mediated responses at the more peripheral level of the cochlea and auditory nerve in experimental animals. While this approach does not directly address the perceptual consequences of such neural activation, it does offer some important and distinct advantages. Physiological evidence (Moxon, 1971; Shepherd et al. 1983) indicates that discrete patterns of hair-cell mediated and direct-nerve excitation can be measured with both single-unit and gross potential measures of auditory nerve activity. Furthermore, experimental data show that these two response classes can, to some degree, be independently controlled through stimulus parameter manipulations. By investigating the phenomena at the peripheral level where they occur, there is a high probability of not only characterizing them, but also exploring effective ways of manipulating them.

Our ultimate goal is to use the physiological data to design listening experiments for human implant users as well as physiological and psychophysical measures to choose appropriate stimulus parameters for users with resid-

ual hearing. In the case of a hypothetical implant candidate with intact apical hair cells, electrical stimulation through basal electrodes will not likely be confined to basal neurons (or those without functional hair cells). Therefore, the response properties of neurons with and without functional hair cell innervation become important. The use of animal models also allows us to more effectively examine the potentially interesting effects of hair-cell mediated responses to electrical stimulation and to lay important groundwork for applications in human implant users.

1.3 Animal models and measures

Our research into auditory nerve responses in cochleae with intact hair cells sought to characterize and manipulate the electrophysiological responses of the mammalian auditory nerve. To that end, we measured both the gross (compound) action potential produced by the whole nerve and single-fiber responses produced by individual fibers. These two types of responses offer the researcher unique advantages and insights into the electrophysiology of the cochlea and auditory nerve.

The gross potential, typically referred to as the electrically evoked compound action potential (ECAP) is recorded by an electrode positioned on or near the auditory nerve. In the case of human implant users, the ECAP can be routinely recorded by the intracochlear electrodes of implant devices equipped with telemetry systems designed for that purpose. The fact that the ECAP can be recorded from both human and research animal subjects makes this measure particularly useful for linking clinical and research findings. As has been demonstrated in previous efforts, animal models of the implanted ear provide significant advantages for our research goals in that they can produce very high quality ECAP waveforms and detailed input-output functions. The animal models also allow us to make careful and extensive manipulations of the stimuli as well as the requisite manipulations of the anatomical status of the cochlea (through experimental deafening techniques).

We have demonstrated that the ECAP is useful for estimating aspects of the population response (Miller et al., 1999b), most notably, the number of active fibers. As it is a summed response, the ECAP does not provide detailed information about temporal response properties (e.g., spike latency and jitter) or single-fiber probabilistic properties. Thus, we have chosen to augment our gross-potential measures with single-fiber measures in order

to examine temporal and probabilistic properties of direct relevance to our hypotheses. Our choices of electrophysiological measures have dictated our choice of experimental animal species. We generally rely on measures from guinea pigs to obtain ECAP measures, while single-fiber measures are obtained from cats, as that species allows recording times adequate for surveys of single-fiber responses. In specific experiments where cochlear anatomy is an important concern (e.g., involving the use of multiple electrode arrays whose dimensions are similar to those used with humans), we have chosen to use cats as our model. All animal experiments were conducted in acute sessions; animals were kept under surgical levels of anesthesia throughout the duration of the experiments.

A key feature of our ECAP experimental design was the use of an acute preparation that allowed for direct within-subject comparisons of electrophysiological responses obtained both with and without functional hair cells. We designed the experiments so that the same electrode configurations (both stimulation and recording) were used within a single experimental session to conduct pre- and post-deafening measurements within the same ear.

Details of general experimental techniques have been outlined elsewhere (Miller et al. 1998, 1999a). The auditory nerve was surgically accessed and recording electrodes placed on the nerve trunk. After initial assessment of acoustic sensitivity, a cochleostomy was performed by drilling a small hole in the bone adjacent to the round window to access the scala tympani of the basal turn of the cochlea. A stimulating ball electrode was advanced through the opening such that the ball was inside the scala but not directly touching the spiral lamina or membranous structures. This approach was used to minimize hearing loss and assure stable stimulating conditions throughout the experiment. A similar approach was used in both guinea pigs (for ECAP recordings) and a limited number of cats (for single-fiber recordings). A micropipette penetrating the nerve trunk was used for recording single-fiber potentials. Details of recording, artifact reduction and analysis have been reported previously (Miller et al. 1999a).

1.4 Descriptions of experimental efforts

To address the aforementioned issues, we have conducted a series of experiments designed to characterize the response patterns with and without functional hair cells as well as to explore the interactions between acoustic and electric stimulation. These experiments are briefly introduced below

and more detailed results from each set of experiments are presented in the following sections.

1.4.1 Effect of functional hair cells on the response to electrical stimulation

Our first set of experiments examined the effects of functional hair cells on the responses of auditory afferent neurons to electrical stimulation. Throughout this work, we used single-pulse stimuli to characterize response growth as well as pulse trains to characterize the time course of refractory recovery and adaptation. We hypothesized that, in addition to electrophonic effects, the presence of synaptic activity from hair cells would have an effect on the direct neural response to electrical stimulation. Measures of activity obtained before and after deafening addressed this issue. Parallel experiments used our computational model of the auditory nerve to investigate the effects of modeled spontaneous synaptic activity on both the electrically evoked compound action potential (ECAP) and single-unit responses to electrical stimulation.

1.4.2 Effect of acoustic stimulation on the responses to electric stimulation

Cochleae with viable hair cells present the possibility of interactions between simultaneously delivered acoustic and electric stimuli. Such interactions can be investigated using a wide variety of acoustic and electric stimuli, and interactions could take the form of masking-like effects as well as synergistic effects. While we typically employed electric pulses, we used several types of acoustic stimuli to assess different aspects of putative electric-acoustic interactions. As an initial assessment, we chose first to use relatively intense wideband acoustic noise to increase random activity of a wide range of fibers and presumably to maximize interactions occurring across that fiber population. We describe other experiments in which we used filtered acoustic noise to assess the spatial characteristics of observed acoustic-electric interactions. We also used a low-frequency acoustic tone to assess the temporal properties of acoustic-electric interactions. Finally, we examined properties of adaptation, to determine how adaptation to acoustic stimulation affects the subsequent response to electrical stimulation.

1.4.3 Responses in ears with partial hearing loss

Our early experimental efforts purposefully used animal models with completely intact hair-cell populations in order to maximize the potential influence of hairs cells on electrically evoked responses and hence, contrasts with measures from deafened ears. However, more clinically relevant issues involve cochleae that exhibit partial loss of the hair-cell complement in a manner that approximates hearing-loss patterns of candidate patients. The goal of this third set of experiments was to determine the extent to which acoustic-electric interactions are manifest in a more realistic animal model - one with partial depletion of the hair-cell population. One would expect that the relative locations of the intracochlear stimulating electrode and the surviving hair cell population would influence the degree of electric and acoustic interaction. Our use of this animal model addressed the question of differential excitation of the apical and basal fibers in a model of limited hearing and attempted to simulate conditions that may be typical of a cochlear implant candidate with residual hearing.

1.4.4 Binaural interactions

The final area of investigation concerns binaural interactions between acoustic and electric stimulation. We approached this question using an animal model with normal hearing on one side and complete loss of hair-cell function on the opposite side. We addressed the integration binaural information in the central nervous system by using the binaural ABR measure, originally defined by the experiments of Dobie and Berlin (1979). While this measure is certainly limited in scope and does not necessarily correspond to binaural perceptual abilities, we view it as a concrete measure of binaural interaction that can be assessed in an animal model. The binaural ABR to acoustic stimulation in both ears of normal hearing animals was used as a baseline. After inducing hair cell loss in one cochlea, the binaural response to various combinations of acoustic and electric stimulation in each ear was assessed.

2 Results

In this section, we summarize the experimental findings of each of the four major research topics that were outlined in the above section.

2.1 Topic 1: Effect of functional hair cells on the response to electrical stimulation

2.1.1 Initial ECAP measures obtained both before and after deafening procedure (QPR1, QPR3)

An early set of experiments involved the collection of ECAP responses (to single-pulse and pulse-train stimuli) in animals both before and after chemical deafening. After placement of electrodes, the acoustic responses to click stimuli were measured and a threshold determined. Responses to various stimulus paradigms were obtained after which an intramuscular injection of kanamycin was administered, followed by intravenous injection of ethacrynic acid (West et al., 1973; Brummett et al., 1979; Xu et al., 1993). The animal's acoustic sensitivity was then re-assessed to assure that no measurable acoustic response was evident. With our equipment, this corresponded to an upward threshold shift of at least 80 dB. ECAP measures were then repeated, providing data for comparisons of response properties with and without functional hair cells. Hair-cell mediated and direct neural responses are separable according to their latency. The electrophonic response, having a latency of about 2 ms, is evident prior to, but not after, deafening. In contrast, the direct neural response, with a latency of less than 1 ms, is evident both before and after deafening but can exhibit a change in amplitude.

Results from these initial experiments were reported in QPR1 and QPR3. The data demonstrated pre- and post-deafening differences in the growth of the response to single electrical pulses. Changes in the ECAP input-output function were evident at relatively low stimulus levels, suggesting that intact hair cells impart an effect at low levels whereby ECAP thresholds are decreased. However, increased sensitivity was not evident at a higher ECAP response amplitude (i.e., 50% of maximum), suggesting that this hair-cell-mediated effect is restricted to relatively low stimulus levels. We also observed changes in the responses to repetitive, pulse-train electrical stimulation in our pre- and post-deafening comparisons. We (Matsuoka et al., 2000) and others (Wilson et al., 1994) have observed patterns of ECAP amplitude alternation in response to pulse trains presented at inter-pulse intervals on the order of 1 ms. In our pre- and post-deafening experiments, we observed an increase in the degree of amplitude alternation after deafening. This change is consistent with a hypothesis of decreased spontaneous activity and correspondingly decreased stochastic response. Finally, the decrease in response over time to the pulse train, or adaptation, was greater before

deafening, presumably due to the effect of hair cell synaptic activity.

2.1.2 Detailed measures of changes over time with hearing loss and recovery (QPR10)

The temporal effects of chemical deafening with combined delivery of a loop diuretic and an aminoglycoside follow a complex course as both drugs produce unique, time-dependent changes in hearing sensitivity (Russell et al., 1979). For example, administration of the loop diuretic can produce a transient loss of sensitivity, while the combined dosing produces a synergistic effect that leads to a permanent threshold shift. We therefore planned follow-up experiments to systematically examine the time course of drug-induced hearing loss and recovery as well as the responses to electrical stimulation over the same time period.

These experiments employed two different drug protocols. QPR10 described a preliminary report of the results with furosemide injections. Those experiments provided an alternative method of transient deafening and also allowed for measures of electrical response after recovery. In QPR10, we described similar trends with kanamycin / ethacrynic acid deafening based on responses in five animals. There was increased amplitude of response, increased alternation and a decrease in the adapted response amplitude. The data relative to recovery after deafening was not as clear, since in many cases, we did not observe recovery to the pre-treatment thresholds.

In this section, we summarize the results of more recent experiments with furosemide treatment examining in more detail the time course of hearing loss and recovery. After implantation, the hearing in each animal was assessed using click stimuli and measuring the acoustically evoked compound action potential (ACAP). Furosemide (typically 80 mg/kg) was delivered intravenously. The ACAP evoked by a fixed, high-level click was measured repeatedly over the course of the experiment, which lasted several hours. A typical pattern of hearing loss and recovery as assessed with the ACAP is shown in Figure 1 (filled symbols).

ECAP responses to electrical stimuli were also assessed over this time course. Initially, a growth function (response to single pulses as a function of stimulus level) was measured in order to characterize the range of effective stimuli for that stimulating electrode. Levels were then chosen to produce response amplitudes at 40%, 60%, 80%, 90% of the saturated response am-

plitude, as well as the lowest level producing the maximum (100%) ECAP amplitude. For each of these levels, ECAP responses were recorded to a train of biphasic pulses (IPI=1 ms; total train duration = 100 ms). Three properties were measured to characterize the pulse-train responses:

1. Response amplitude to the first pulse in the train (i.e., the unadapted response)
2. Alternation amplitude, defined as the average difference in responses to adjacent pulses for the 10th through 19th pulses in the train
3. Adapted amplitude, defined as the average asymptotic ECAP amplitude averaged from a response epoch from 80 to 99 ms. Adapted amplitude is expressed relative to the ECAP amplitude evoked by the first pulse in the train

These three measures are plotted in Figure 1a-c, respectively. In each case, the ECAP amplitude before deafening (relative to ECAP dynamic range) is the parameter. The responses over time show trends typical of the group data. After onset of hearing loss, there is a tendency for first-pulse response amplitude to increase (Figure 1a), alternation amplitude to increase (Figure 1b) and adapted amplitude to decrease (Figure 1c). After recovery there is a tendency for those trends to reverse.

The trends observed in the example data of Figure 1 were quantified for each of eight guinea pigs and summarized in Figures 2, 3, and 4, for measures of first-pulse response amplitude, amplitude alternation, and adapted amplitude, respectively. Shown along the abscissa are three different comparison conditions of hearing status. The first condition ("deaf1/hear") compares measures obtained just after initial deafening to the pre-deafening measure. The second condition ("recover/deaf1") compares measures obtained after the ACAP recovered to at least 95% of the pre-deafened amplitude. Finally, in some animals, a second furosemide dose was given, providing us with a second deaf period and a third comparison condition ("deaf2/recover"). Figure 2 plots the unadapted (first-pulse) response, Figure 3 plots results for the alternation amplitude and Figure 4 plots adaptation amplitude. In each figure, the five graphs show response ratios for five response amplitudes chosen to span the dynamic range of the ECAP. The results show trends similar to those reported above: With hearing loss, unadapted response amplitude

and alternation amplitude tend to increase and adaptation amplitude tends to decrease.

Effects of response amplitude on these three measures are illustrated in Figure 5. The largest effects on alternation and adaptation tend to occur at higher response amplitudes. There is also a tendency for the largest effects on unadapted response to occur at levels producing responses in the middle of the dynamic range.

2.1.3 Electrophonic effects

The data described in the two previous sections summarize effects of hair cells on direct neural activation through electrical stimulation. Another mode of excitation - the electrophonic response - is distinguished by its long latency and vulnerability to insult to the hair-cell population (Moxon, 1971). We have conjectured that an electrophonic response could be beneficial, particularly in increasing dynamic range and jitter in the temporal response to electric pulses. However, when pulse-train stimuli typical of a cochlear implant are used, significant temporal overlap between the direct and electrophonic responses may occur as a result of their latency differences. Figure 6 illustrates the response of a single fiber of a deafened cat to pulse train stimulation. The train consisted of seven equal-amplitude pulses separated by an interpulse interval (IPI) of 1 ms. Responses are shown as a dot display, depicting spike times across the stimulus presentation epoch. The high degree of synchrony observed is typical of neurons in a deafened ear, as are different response probabilities to successive pulses, presumably due to refractory effects. These single-fiber response patterns are consistent with those observed in ECAP responses.

Figure 7 presents dot rasters from a fiber with acoustic sensitivity, as determined from both ACAP measures and the fiber's spontaneous activity. Responses to a single electric pulse are shown in Figure 7-A. This fiber has significant spontaneous activity as well as a particularly clear electrophonic response that occurs between 1 and 2 ms. As has been reported previously (Moxon, 1971, Shepherd et al., 1983; van den Honert & Stypulkowski, 1984), the electrophonic response has a low threshold and a low rate of growth. In this case, the direct response is only evident at high stimulus levels (less than 1 mA) compared to the electrophonic threshold near 0.15 mA.

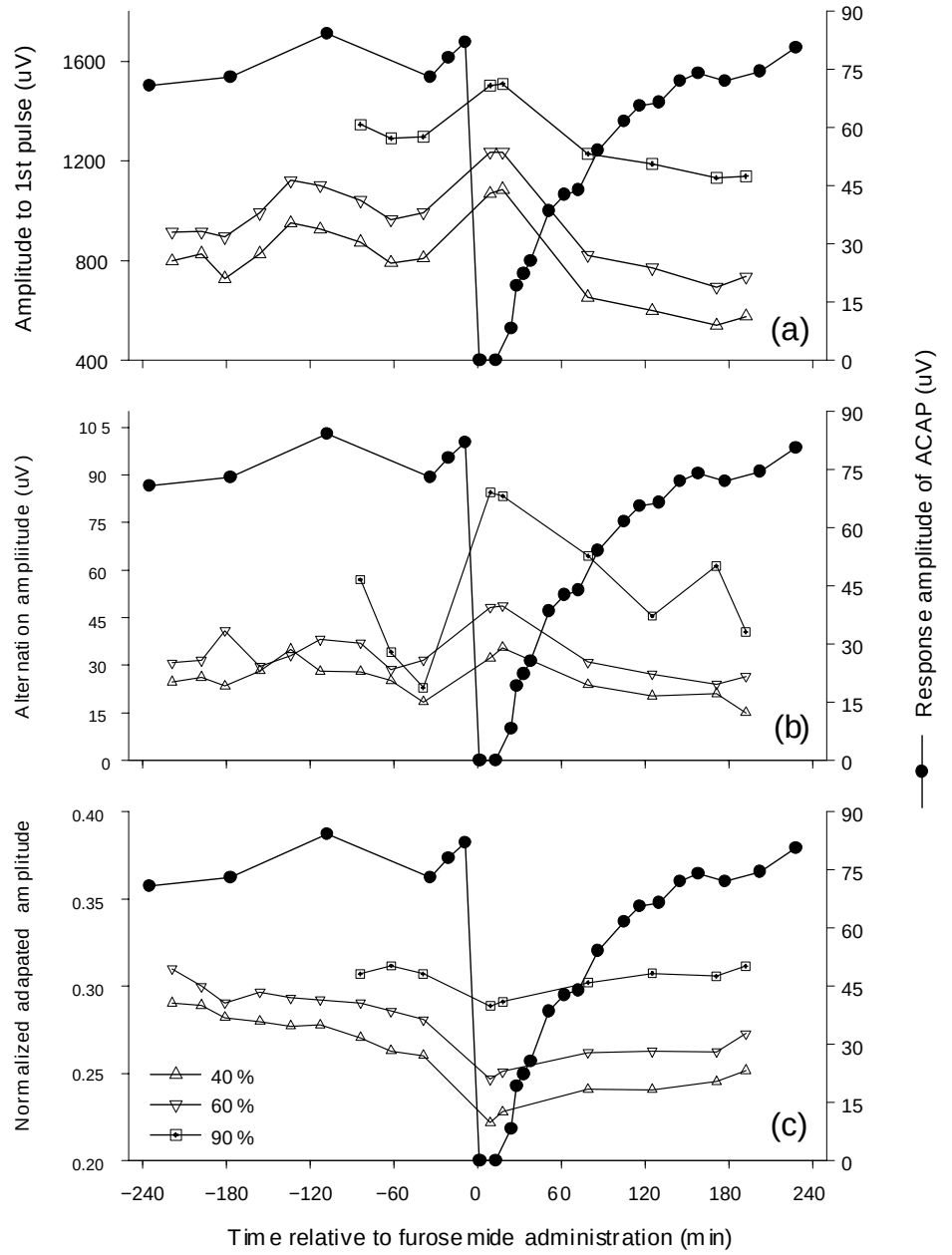

Figure 1: The time course of the response to the first pulse (unadapted response) (a), alternation amplitude (b) and normalized adapted amplitudes (c) in response to the electric pulse train are plotted as a function of time relative to the administration of furosemide (subject M24). The stimulus levels for pulse train were chosen from the ECAP growth function in response to the single pulse to produce response amplitudes at 40%, 60% and 90% of the saturation in this subject before furosemide teatment as indicated by the symbols. The response amplitudes of ACAP were monitored with a fixed, high level of click and are plotted with filled symbols over the same time course.

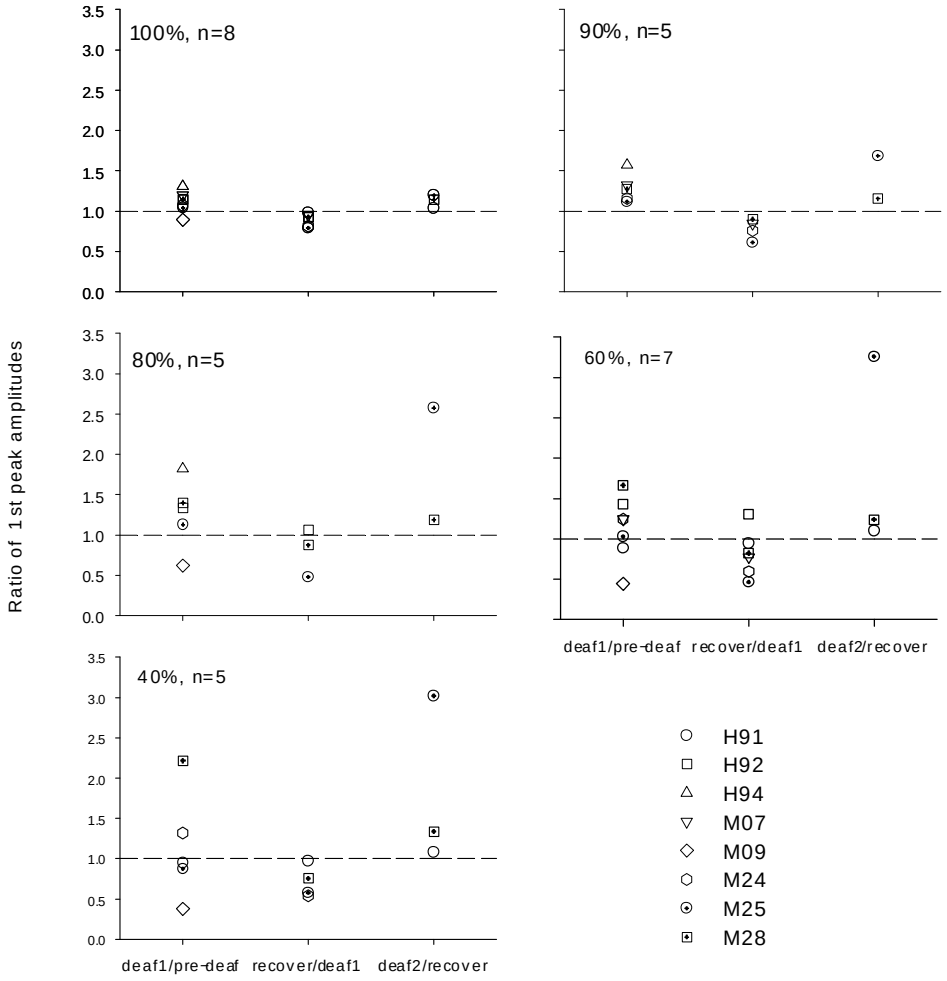

Figure 2: The ratios of the amplitude of response to the first pulse in the train are plotted for different conditions: before and after deafening (deaf1/pre-deaf), after recovery of hearing relative to initial deafened condition (recover/deaf1) and before and after the second deafening procedure (deaf2/recover). Each plot shows data for a signal level which elicits a specified response amplitude expressed in terms of the ECAP dynamic range. Each graph summarizes data from several animals, indicated by the symbols.

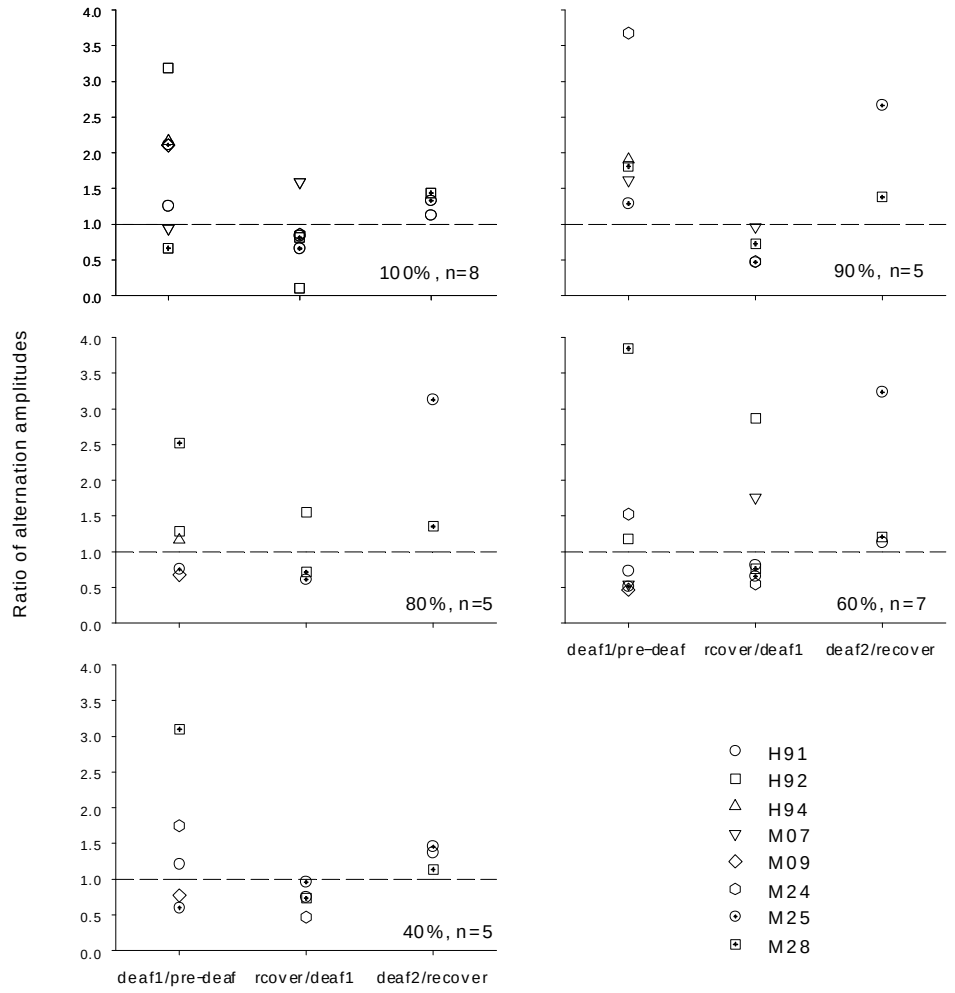

Figure 3: The ratios of the alternation amplitude (see text) of response to the pulse train are plotted for different conditions: before and after deafening (deaf1/pre-deaf), after recovery of hearing relative to initial deafened condition (recover/deaf1) and before and after the second deafening procedure (deaf2/recover). Each plot shows data for a signal level which elicits a specified response amplitude expressed in terms of the ECAP dynamic range. Each graph summarizes data from several animals, indicated by the symbols.

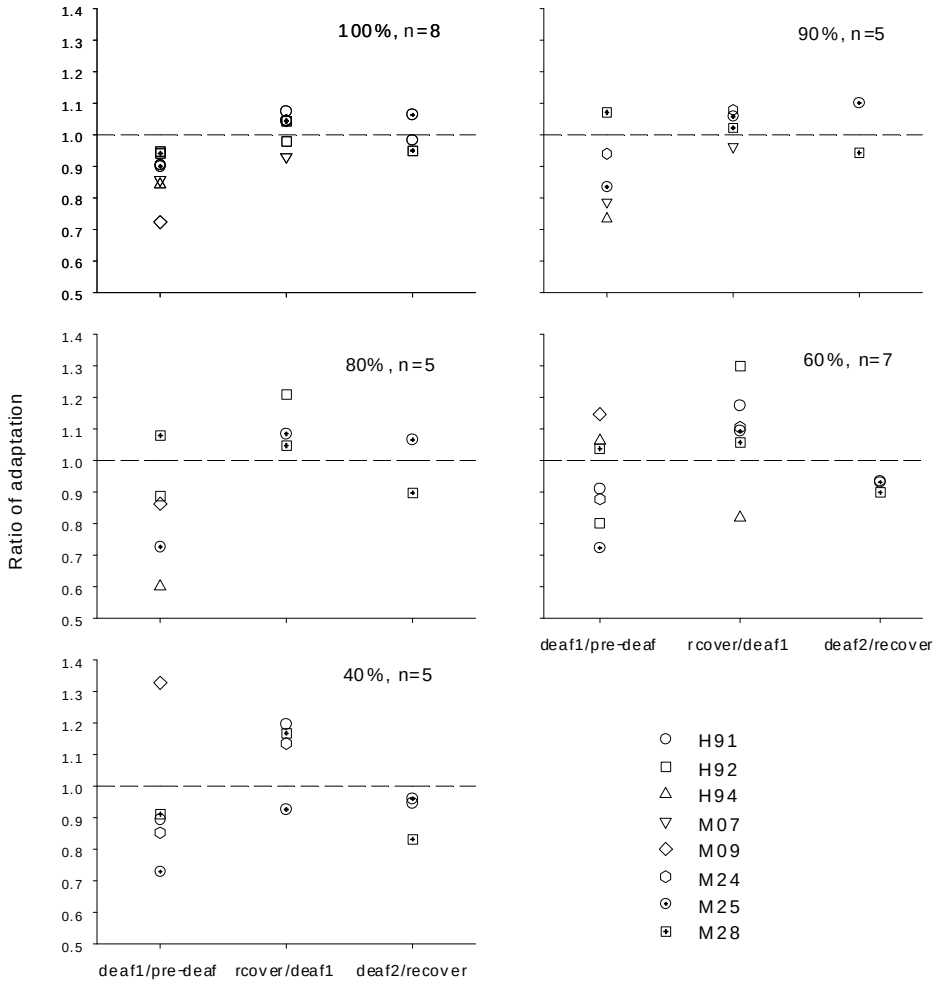

Figure 4: The ratios of the adaptation amplitude of response to the pulse train are plotted for different conditions: before and after deafening (deaf1/pre-deaf), after recovery of hearing relative to initial deafened condition (recover/deaf1) and before and after the second deafening procedure (deaf2/recover). Each plot shows data for a signal level which elicits a specified response amplitude expressed in terms of the ECAP dynamic range. Each graph summarizes data from several animals, indicated by the symbols.

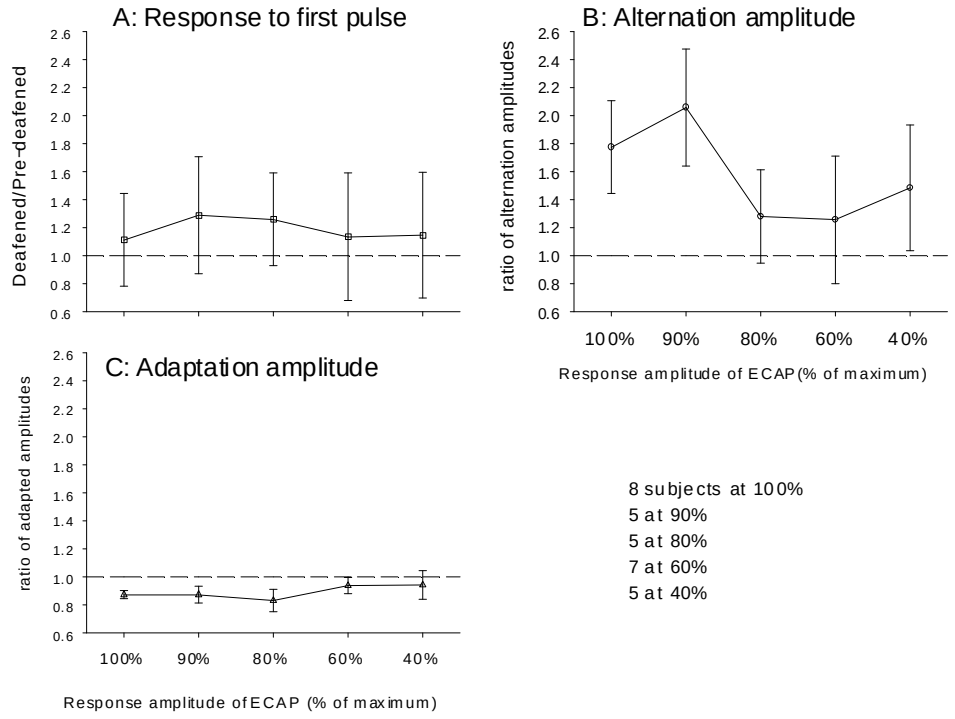

Figure 5: The mean value and standard error of the ratio of responses before and after deafening (deafened/pre-deaf) are plotted as a function of stimulus response amplitude expressed as a percentage of the ECAP dynamic range. A shows data for the response to the first peak, B shows data for alternation amplitudes and C shows data for adapted amplitudes. The number of animals for each level (group) is indicated in the legend.

Interpretation of the responses of the same fiber to an electric pulse train (Figure 7B) is not as straightforward. At low stimulus levels, the response to the first pulse occurs after the presentation of the second pulse. At high levels, the direct response to the second pulse can overlap the electrophonic response to the first pulse. The resulting response consists of a combination of direct and electrophonic responses. Nevertheless, compared with the response from the "deaf" fiber (Figure 6), this response pattern demonstrates both greater jitter and a much greater dynamic range.

2.1.4 Model simulation (QPR2 and QPR6)

We incorporated a model of the inner hair cell synapse into our computational biophysical nerve-fiber simulations to better understand the experimental results summarized above. We found that, as expected, a deterministic neuronal membrane model is adequate for synaptic simulations as long as the synaptic noise is much greater than the neuronal membrane noise. For example, coupling a deterministic membrane model to a synaptic model is adequate to predict that responses to low-frequency sinusoidal electrical stimulation have improved temporal resolution in the presence of physiologic levels of spontaneous activity. However, for stimulus paradigms likely to result in the development of significant membrane noise, such as with high-rate pulse trains, both a stochastic membrane model and a stochastic synaptic model (i.e., a "bi-stochastic" model) are necessary in order to accurately predict response properties.

We have used this "bi-stochastic" model to analyze the effects of fiber threshold distribution, membrane noise and synaptic noise on responses to prolonged pulse trains, and found that it can explain many characteristics of these responses in both humans and experimental animals. Fiber threshold distribution acts as a third "noise source" and is comparable to a random current increment added to the stimulus. The ongoing "alternating pattern" of ECAP amplitudes seen in human subjects in response to pulse trains represents an interaction between refractoriness and the threshold distribution (Figure 8); without the effects of threshold distribution, the "alternating pattern" would be all or none. These results suggest that threshold distribution is the dominant noise source in the chronically deafened human ear.

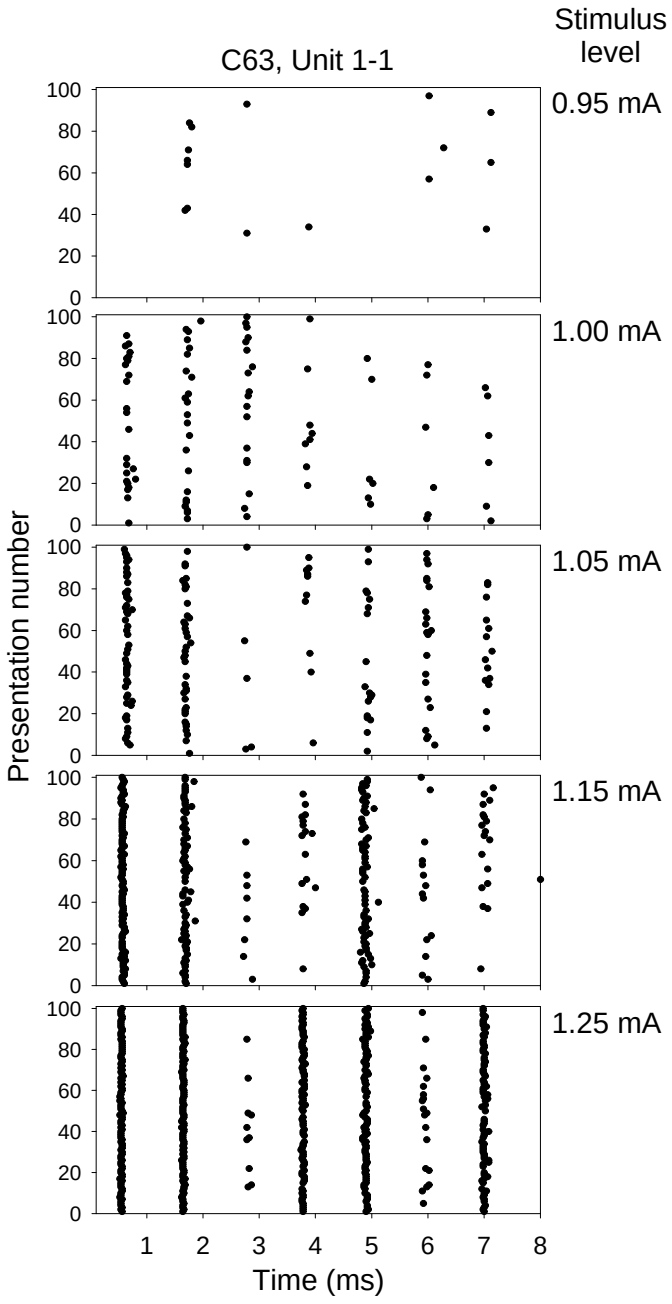

Figure 6: Single fiber response to pulse trains in an animal with no functional hair cells. Stimuli were seven biphasic pulses, 40ms/phase, IPI 1 ms.

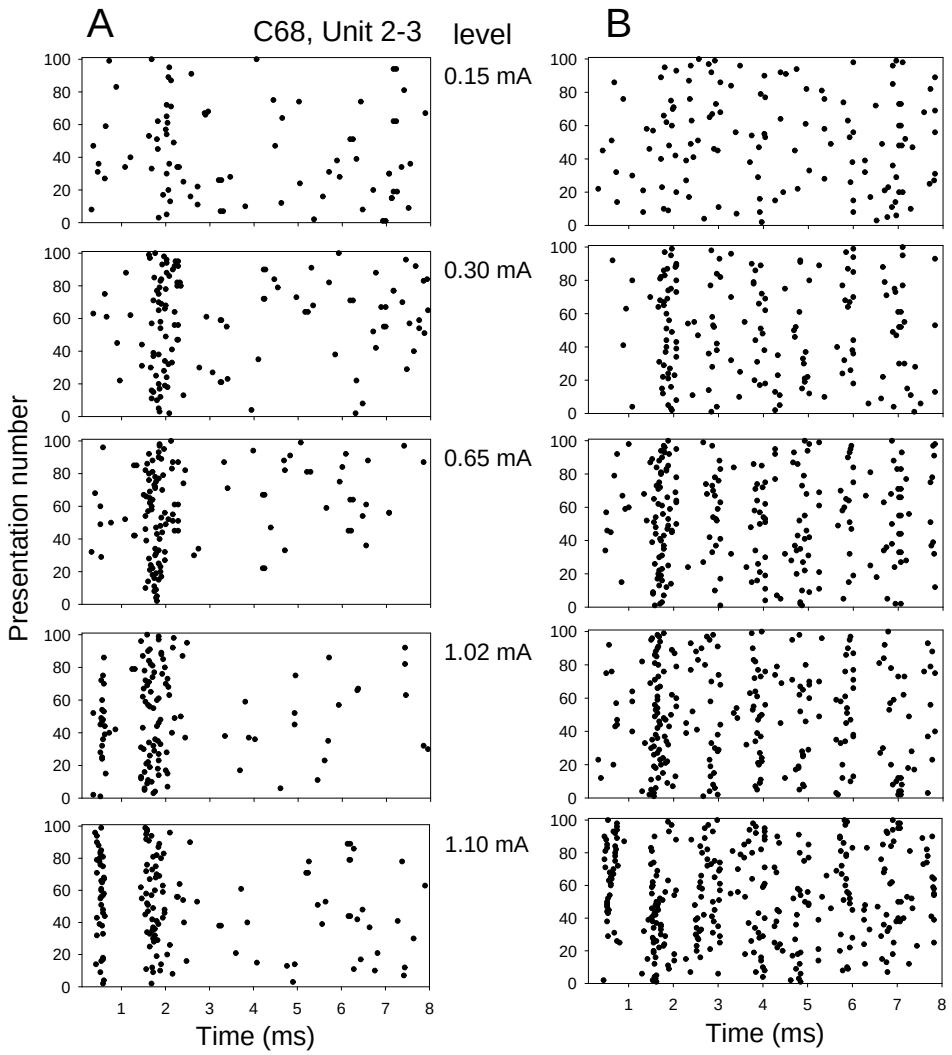

Figure 7: (A)Single fiber responses to single pulses in an animal with functional hair cells and significant electrophonic response. Stimulus single biphasic pulses, 40ms/phase, IPI 30ms. (B) Stimuli were seven biphasic pulses, 40 ms/phase, IPI 1 ms.

Model manipulations that increase synaptic or membrane noise cause an increase in the rate of decay of response alternation, consistent with our animal data. The larger the synaptic or the membrane noise, the faster the decay occurs (Figure 9). Comparison of ECAP responses to pulse trains in humans and animals suggests that acutely deafened animals possess significantly more intrinsic membrane noise than do chronically deafened humans. A loss of the peripheral fiber processes in chronic deafness could underlie this finding.

Lastly, we have examined the effects of synaptic noise on the amplitude of the ECAP during the onset of a pulse train. Increasing synaptic noise leads to an overall decreased ECAP onset amplitude much as has been seen in the experiments described above. Thus in multiple measures, the "bistochastic" model demonstrates that our qualitative interpretation of the effects of spontaneous activity on responses to electrical stimuli are correct and are consistent with physiologic levels of stochastic intensity at the inner hair cell synapse.

2.2 Topic 2: Effect of acoustic stimulation on the responses to electrical stimulation

The results of the experiments of Topic 1 describe the effects of functional hair cells on the response to electrical stimulation. We conjecture that part of these effects may be due to increased spontaneous synaptic activity present in the hearing preparations. Those findings motivated a study using externally generated acoustic stimuli to determine how the addition of acoustic energy may alter evoked responses. We have used various wideband and sinusoidal acoustic stimuli to assess the ability of exogenous stimuli to interact and alter ECAP responses. Some of this work was motivated by that of Moxon (1971) who demonstrated that interaction of acoustic and electric stimuli could be observed at the level of the single-fiber.

2.2.1 Effects of wideband acoustic noise (QPR5)

Our first and most basic experiments investigated the effect of wideband acoustic noise on ECAP responses. A wideband (20 kHz) gaussian noise generator was used to drive an earphone coupled to the guinea pig external ear canal. Noise was presented continuously throughout data acquisition

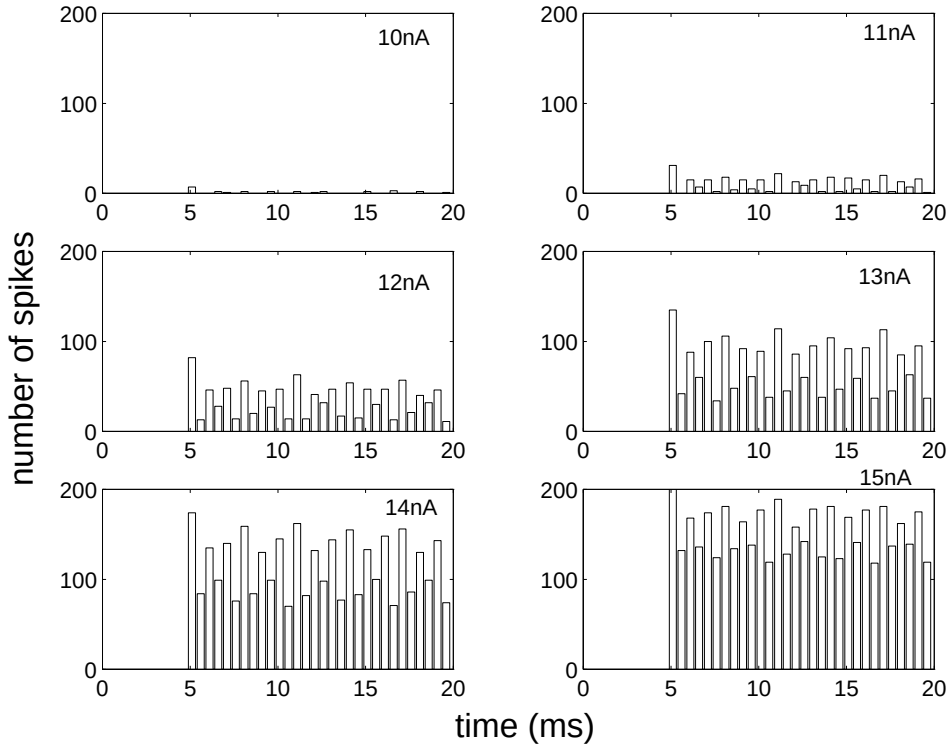

Figure 8: Post-stimulus time histograms obtained by simulating the excitation of 100 uniform deterministic nodes of Ranvier with a 14 nA electric sinusoid. The onset of the sinusoid occurs at t-5 ms. The parameter is the level of synaptic current.

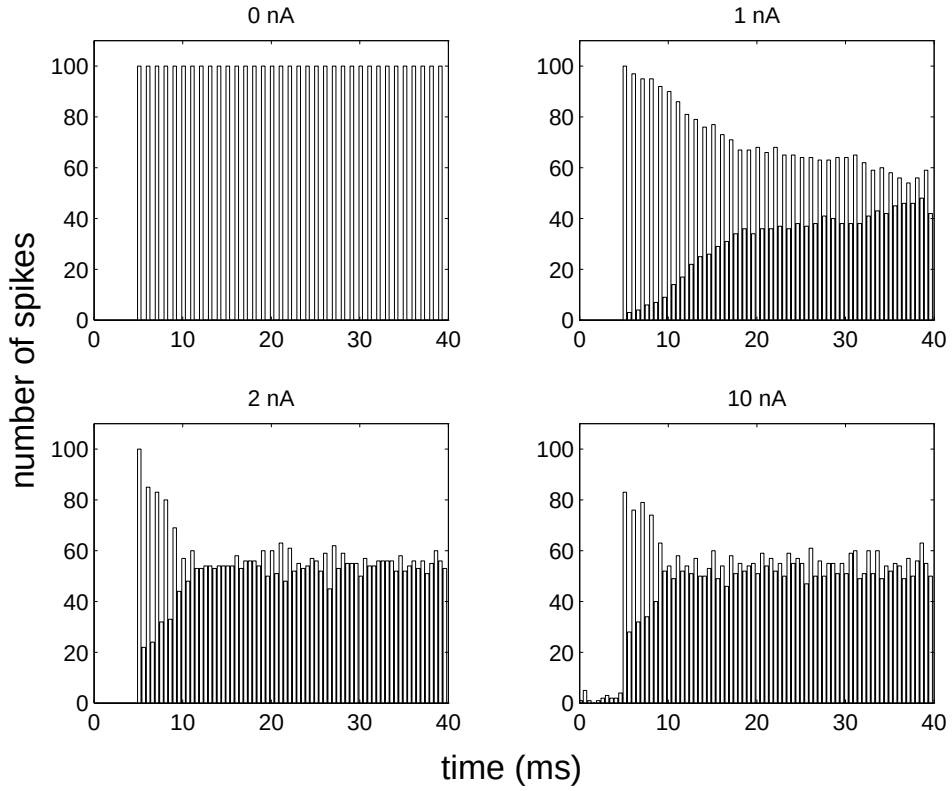

Figure 9: A series of 6 post-stimulus-time histograms obtained by simulating the excitation of 200 deterministic nodes of Ranvier at different current levels (indicated by the parameter). In these cases, there is no synaptic current. The electric stimulus is a 2 kHz sinusoid with its onset occurring at 5 ms. The nodes have a range of thresholds with standard deviation 20 percent.

at a maximum overall level of approximately 100 dB SPL. Figure 10 illustrates the effect of wideband acoustic noise on ECAP growth for two guinea pig preparations. Plots in the left column show growth functions for both masked and unmasked conditions; plots in the right column show the masked growth functions normalized to the amplitudes obtained without masking. The data of both animals show trends typical of the population studied to date. Over a wide range of electric levels, acoustic masking reduces the amplitude of the evoked response, with the largest proportional response occurring at low-to-middle current levels. Generally, the magnitude of the response decrement is about 10-20%; however, these decrements become smaller as the stimulus is reduced to low levels. In some cases, there appears to be an increase in the ECAP at the lowest electric levels. However, these low-level responses also demonstrate increased variability across the different levels of the acoustic stimulus, suggesting that the apparent enhancements in the ECAP may be artifactual. The relatively poor signal-to-noise conditions inherent in responses obtained at the lowest stimulus levels may produce sufficient variability in the measured responses such that some of the relative response measures produce ratios greater than one. This low-level region is clearly relevant to prosthetic stimulation and will be investigated in more detail in future work. Due to possible limitations inherent in recording low-level, averaged potentials, the use of single-fiber measures is suggested.

2.2.2 Effects of sinusoidal acoustic stimuli, phase effects (QPR5)

We have also investigated the interaction of electric stimuli with an acoustic stimulus presented as a continuous sinusoid. Using tonal acoustic stimuli, we can examine the influence of the phase of the acoustic stimulus relative to the time at which the electric pulse is presented. A high level 100-Hz tone is presented continuously to the ear through a speculum attached to the external canal. ECAP responses are then evoked by a single biphasic stimulus pulse delivered at different specific phases relative to the sinusoid. The level of the tone and the electric pulse are also systematically varied, and separate time-averaged ECAP responses are obtained for each of six phases.

The interaction between tone and electrical pulses are shown in the plots of Figure 11, where ECAP amplitudes are plotted as a function of the relative phase of the electric pulse and the pulse level. Note that "relative phase"

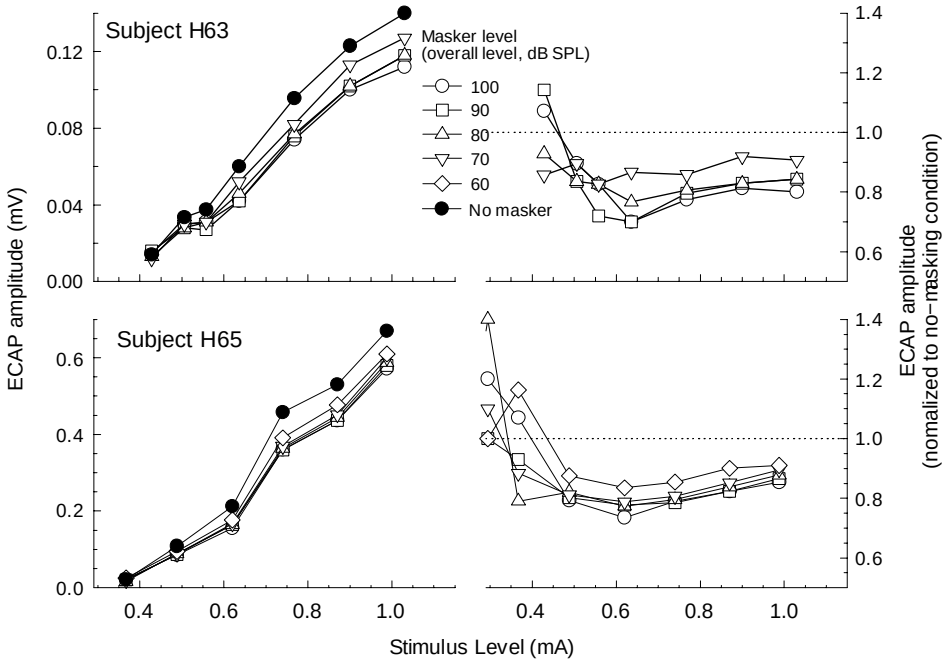

Figure 10: ECAP amplitude-level functions obtained from two guinea pigs preparations demonstrating the interaction of electric and acoustic stimulation. The electrically evoked responses were obtained using 40 microsecond/phase biphasic current pulses. Wideband acoustic noise stimuli were delivered to the same ear through an earphone and speculum sealed to the external auditory meatus. The overall sound pressure of the noise is indicated by the symbol type and legend.

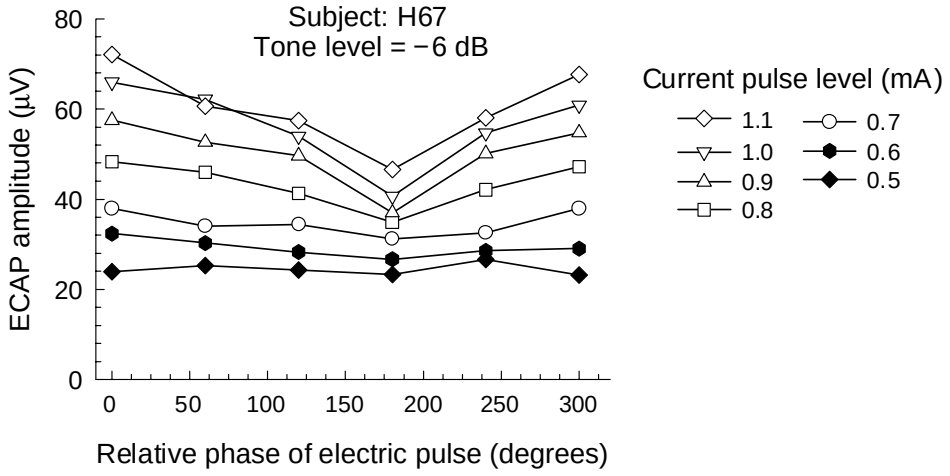

Figure 11: Results of the acoustic tone and electric pulse interaction studies conducted in two guinea pig preparations. ECAP amplitudes are plotted as a function of the relative phase of the electric stimulus pulse, with the pulse level shown as a parameter. The pulse stimulus levels were chosen to span the dynamic range of the ECAP amplitude-level function.

does not indicate the phase relationship between the tone and pulse at the basilar membrane, as we have not accounted for sound propagation delays. Tone and electric pulse interactions are observed at only the highest level of the tone stimulus (i.e., between 85 and 95 dB SPL). Furthermore, the phase effects are greatest at the higher levels of the electric stimulus. To date, we have not observed any interactions between the phase and stimulus levels.

We have also compared these phase-specific responses relative to ECAP amplitudes produced without the simultaneous acoustic tone. To date, we have only reliably observed phase-specific decrements in the ECAP with acoustic stimulus and have not observed any ECAP enhancement effects. Again, this may be a limitation of the specific (time-averaged, gross-potential) measure.

2.2.3 Effect of spectral content of noise (QPR7)

We have collected responses to electrical pulses (delivered through a monopolar electrode in the base of the cochlea) with various high-pass filtered, acous-

tic noise stimuli as maskers. In all cases, the spectrum level of the noise was held constant as the high-pass cut-off frequency was varied across stimulus conditions. By manipulating cut-off frequency with high-pass filtering, we could alter the basal-to-apical extent of the fiber population affected by the acoustic noise.

The output of a wide-band (100 kHz) gaussian noise source was fed into an adjustable brick-wall (120 dB/decade) filter to provide a range of noise bandwidths. With no filtering (i.e., using the full bandwidth of the noise), a 96 dB SPL overall level was presented to the ear canal. For each animal, the electric pulse level was adjusted to a level that evoked a response near the middle of the growth function when no acoustic noise was present. ECAP responses were then obtained for several noise bandwidths. Results from six guinea pigs are plotted in Figure 12 as a function of the high-pass cut-off frequency, with amplitudes expressed relative to the that obtained in the no-noise condition. The degree of masking for the wide-band condition varies somewhat across subjects. Nevertheless, for all subjects, the degree of masking changes little for cut-off frequencies up to 3-4 kHz. In contrast to this plateau region, a steep change in masking is observed for cut-off frequencies above 10 kHz. This trend is consistent with a hypothesis that masking is effective only for the basal fibers, suggesting that those fibers are primarily contributing to the response to electrical stimulation.

These ECAP data suggest a limited area of effective masking of electrical stimulation. The results have, in part motivated work described in Section 4 which has used animals with limited hair-cell loss in order to simulate a more realistic model of clinical cases. In addition, we have identified future work to investigate these interactions with single-fiber measures that avoid the possible ambiguities attendant with interpretation of ECAP measures.

2.2.4 Effect of noise on the response of single fibers to pulse trains

The changes observed with the ECAP measurements in the presence of acoustic noise are consistent with an increase in the stochastic properties of the response to electrical stimulation in the presence of acoustic stimulation. Single-fiber responses to combined acoustic and electric stimulation support this notion. The following examples are from a cat using our standard single-fiber recording techniques (Miller et al., 1999a) except that the acoustic sensitivity has been preserved and acoustic stimulation used in addition to

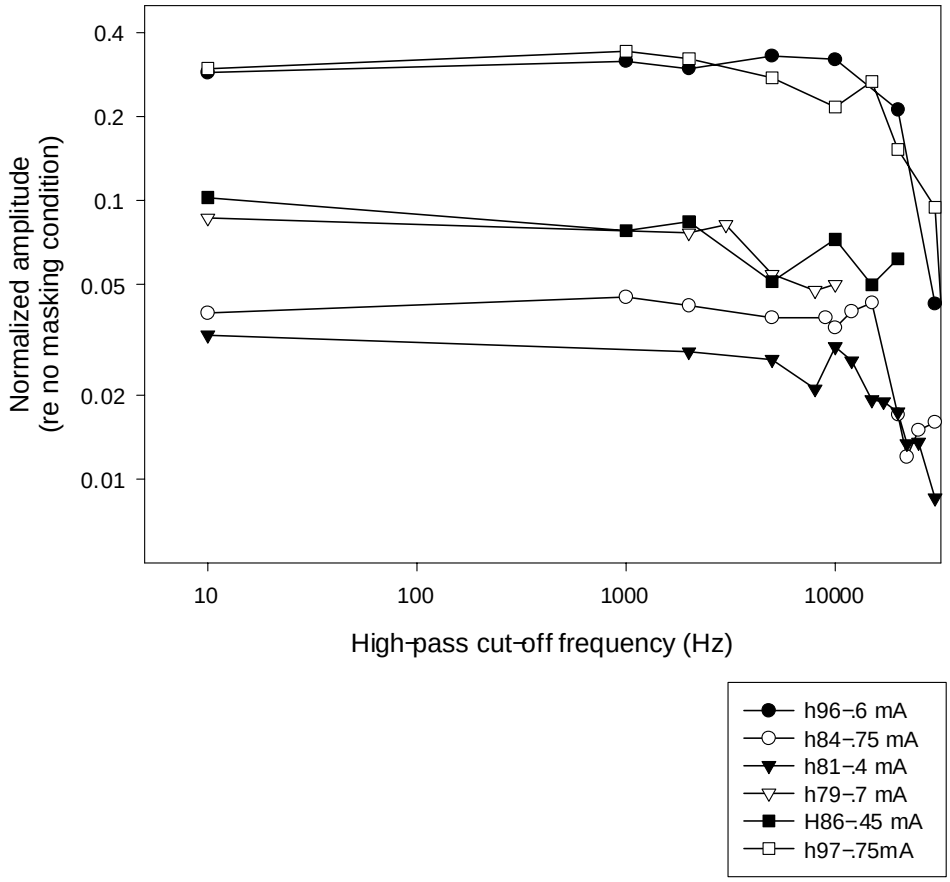

Figure 12: Derived amplitude of response (see text) is normalized to the response to the same pulse without acoustic masking and plotted as a function of high-pass noise cut-off frequency.

biphasic electrical pulses. Figure 13 shows response times for single-fiber action potentials in response to trains of seven pulses presented at an inter-pulse interval of 1 ms. The two dot displays in the left column show responses to 100 repeated trains, both with (bottom) and without (top) presentation of a continuous wideband acoustic noise. The addition of acoustic noise results in an increase in jitter as well as a decrease in refractory effects as assessed by the alternation of responsiveness to successive pulses. This is illustrated in the graph at the right showing spike counts in response to each pulse in the train for both the noise and no-noise conditions.

The increased jitter and reduced refractory effects observed with acoustic noise are also accompanied by changes in the electric rate-level functions. Figure 14 plots total spike count as a function of stimulus level for a fiber both in quiet and with two different levels of background acoustic noise. The lower rates-of-growth at high noise levels are also consistent with increased stochastic response in the presence of acoustic noise. These results suggest a possible benefit of electric-acoustic interactions in the acoustically sensitive, implanted ear, as acoustic noise may be able to counteract, to some degree, the very small electrical dynamic range observed in the deafened ear. This research area deserves further attention.

2.2.5 Adaptation effects with acoustic noise (QPR7)

In examining acoustic-electric interactions, we have used wide-band noise stimuli at levels up to 100 dB SPL (overall level) with durations on the order of one minute. Such stimuli can have a clear effect on the subsequent responsiveness of fibers to sound stimuli (Young and Sachs, 1973). In collecting the data with acoustic noise, we noted that the changes in the ECAP varied over the duration of the acoustic masker. In addition, the recovery to "unmasked" response amplitude was not immediate, i.e., the recovery took place over several seconds.

The time course of these changes is illustrated in Figure 15. ECAP amplitude in response to a 0.7 mA biphasic pulse is plotted as a function of time. Each point represents the response amplitude based on the average of 20 stimulus presentations, many fewer than usual for our ECAP recordings. As a result, the amplitude measures are noisy and exhibit significant variability across the data set. We used this relatively low number of recordings-per-average to better track temporal changes in ECAP ampli-

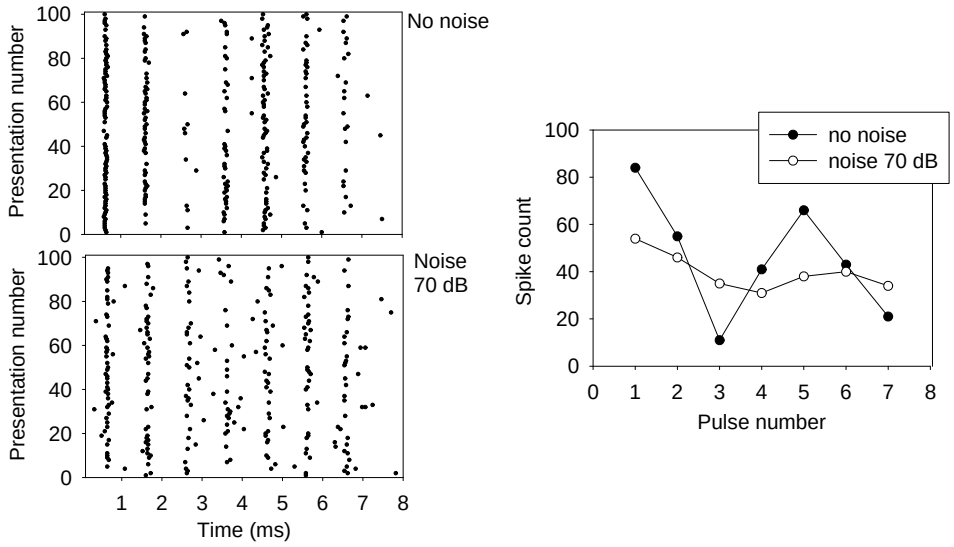

Figure 13: Single-fiber responses to electric pulse trains with and without continuous background noise.

tude. During data collection, a 96 dB SPL wide-band noise was presented at the times indicated on the graph by the horizontal bars. For both noise presentations, there is a relatively fast (approximately 10 s) decrease in the response amplitude after which it reaches an approximate steady state. After the noise is turned off, the recovery to pre-noise response amplitude is not immediate. In these cases, the recovery time is on the order of one minute.

The latencies of the ECAP responses were in the 0.2 - 0.3 ms range, clearly indicating that the responses were not electrophonic in origin, but rather a result of "direct" depolarization. Nonetheless, the responses were affected by the acoustic noise, possibly due to increases in synaptic activity. Even after the noise was turned off (and after cessation of driven synaptic activity), the effect of the acoustic stimulus persisted for some time. This relatively slow time course of recovery suggests a metabolic process, although these measures cannot identify the specific site or mechanism.

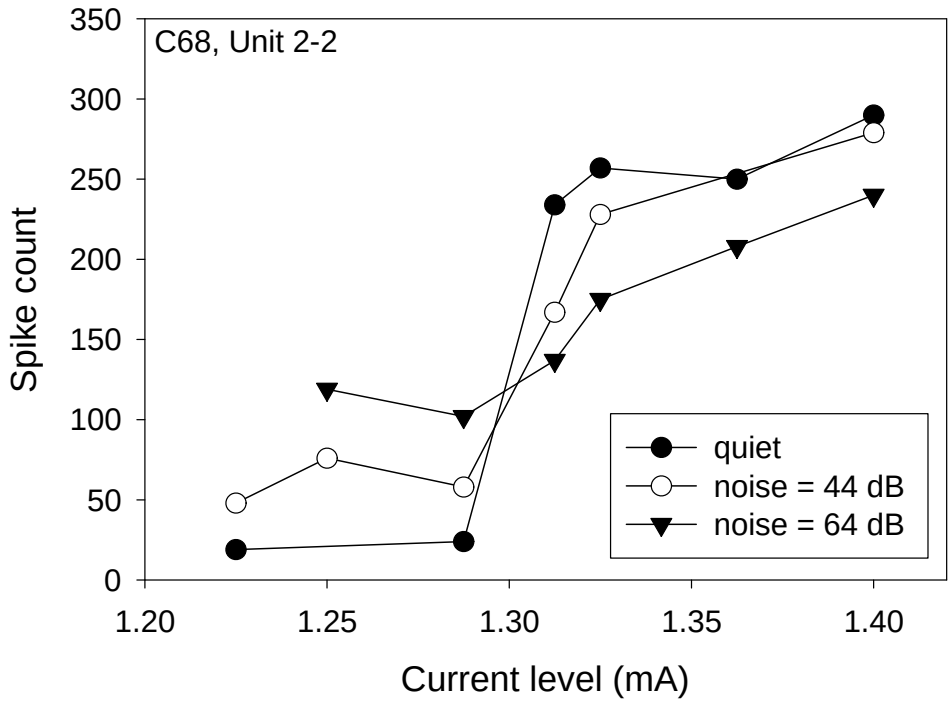

Figure 14: Growth of single-fiber response rate to electric pulse trains with and without continuous background noise.

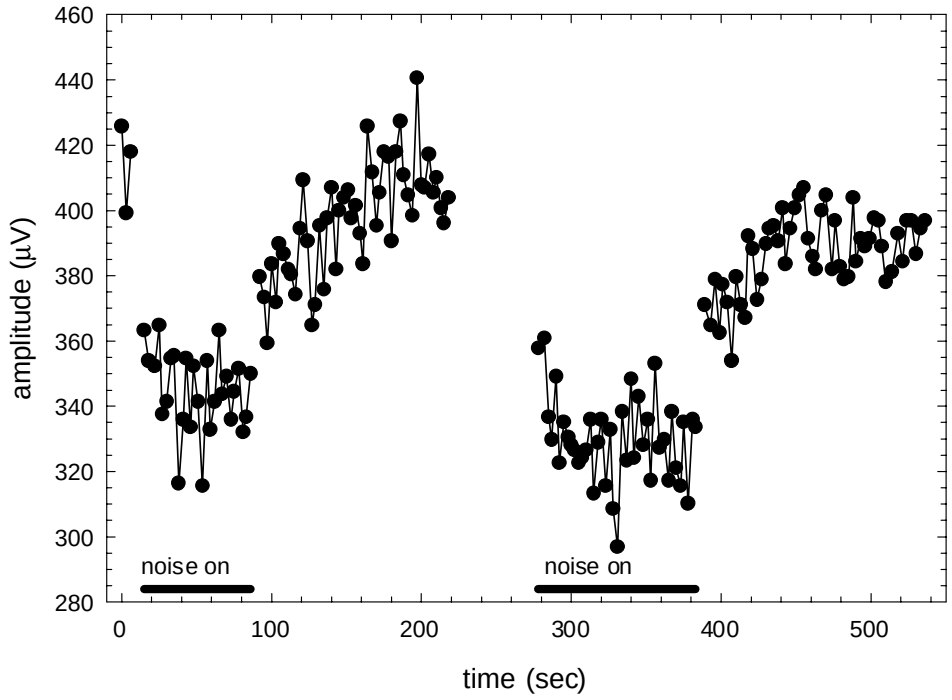

Figure 15: ECAP amplitude in response to a 0.7 mA biphasic pulse is plotted as a function of time. Each point represents the response calculated on the basis of 20 stimulus presentations. Wide-band noise masking at 96 dB SPL is turned on at times indicated by the bars along the abscissa.

2.3 Topic 3: Responses in ears with partial hearing loss

Previous experiments addressed the issue of how the presence of acoustic excitation through hair cells can affect the responses of neurons to electrical stimulation. This section summarizes the work using partially deafened animals to examine the extent to which previous results apply to an ear with high-frequency sensorineural hearing loss. This animal model is an attempt to simulate the type of high-frequency hearing loss that may be typical of an individual receiving a cochlear implant.

Preliminary results and methods used in these experiments were recently described in QPR11. The treated animals displayed significant high-frequency hearing loss 2-3 months after treatment with kanamycin injections. Recently we have begun histological analysis of the treated ears. This analysis was done on the six animals for which we have physiological recordings as well an untreated control. To date, we have completed quantitative analysis at two cochlear locations, 25% and 50% of the length measured from the base. We have examined slides with particular interest in the organ of Corti, spiral lamina and Rosenthal's canal.

2.3.1 Histological evaluation

Methodology

The procedures for histological preparation closely followed those used by Miller et al. (1994). After fixation, each specimen was rinsed in phosphate buffer and the otic capsule thinned with a diamond burr to enhance absorption of subsequent solutions. The specimens were then post-fixed in 1% phosphate-buffered osmium tetroxide with 1.5% potassium ferricyanide, decalcified in 0.1M EDTA, dehydrated, and embedded in an epoxy resin (Spurr, 1969). Subsequent dissection followed the block-surface method of Spoendlin and Brun (1974), a process enabling the assessment of cross sections along multiple orthogonal planes. Accordingly, we took care to preserve the spiral ganglion, organ of Corti and scala tympani in the surface preparations, which were then mounted on glass slides. The length of each cochlea was measured along the apical aspect of the pillar cells and longitudinally partitioned into ten regions, each 2 mm long, beginning at the hook region. From each region, a 0.5 mm thick radial segment of basilar membrane and associated spiral ganglion was removed with cuts made parallel to the radial nerve fibers. Sections (1 micron thick) were then cut in the radial plane (Leake and Hradek, 1988), each containing a sample of Rosenthal's canal, the associated organ of Corti, and scala tympani. Groups of con-

secutive sections, separated by 40 micron intervals, were mounted, stained with Azure B and methylene blue, and examined with a Nikon Labophot light microscope. Since each group of sections is separated from the next by at least 40 microns, no two groups contain common spiral ganglion cells. This procedure yielded approximately 10 sample groups from each 0.5 mm segment.

A complete assessment of each cochlea calls for the examination of ten sample groups from each of the 10 regions and evaluation of the condition of the organ of Corti, the peripheral processes, and spiral ganglion cell density. Cell density measures were made using a point-counting procedure (Weibel, 1979) that we have employed previously (Miller et al., 1994). As of this report, we have completed evaluation of two of ten of the cochlear regions, specifically, those located at 25% and 50% of the baso-apical length relative to the base. These two regions correspond approximately to best-frequency regions of 16 kHz and 4 kHz respectively (Liberman, 1982). Data have been analyzed for each experimental animal and one control. The volume ratio of spiral ganglion cells was determined and counts from 10 sections were averaged to arrive at estimates for each 0.5 mm segment. These average values comprise a single spiral ganglion cell density estimate for each of the selected cochlear sites along its longitudinal (basal-apical) dimension. All tissue slides were coded so that the investigator was blind to the identity of each specimen.

The organ of Corti was evaluated for the presence of hair cells and the condition of the supporting cells as described by Leake et al. (1991). Numbers were assigned to indicate the following conditions: 4, normal pillar cells and maintenance of the cytoarchitecture of the organ of Corti; 3, pillars obviously altered but the tunnel of Corti still recognizable; 2, the organ of Corti collapsed and the tunnel consolidated; 1, complete resorption of the organ of Corti to a single squamous cell layer. The number and condition of peripheral dendrites were determined qualitatively in each section.

Results

Figure 16 provides photographic comparisons of sections of through the organ of Corti and spiral lamina for untreated control (A) and aminoglycoside-treated (B) animals evaluated at the 16 kHz location of the cochlea. A comparison of control (C) and treated (D) sections at the 4 kHz cochlear level is also provided by Figure 16. In both figures, hair cell damage is evident in the treated animals, as well as some reduction in the density of peripheral

processes in the spiral laminae. We expect that the loss of hair cells will result in spiral ganglion cell degeneration in the basal region of the cochlea (Spoendlin, 1975; Kiang et al., 1976; Leake-Jones et al., 1982). We view some degeneration as desirable in that it may better simulate conditions in potential cochlear implant candidates. Such degeneration is evident in the micrographs shown in Figures 17 and 18, which present spiral ganglion cross-sections in control (A) and aminoglycoside-treated (B) animals at both the 16kHz and 4kHz cochlear locations.

The ratings of the organ of Corti and the estimates of spiral ganglion cell density for the two cochlear locations that have been analyzed to date are shown in Figure 19-A and 19-B. The measured hearing loss in those ears at the time of data collection (pre-deafening ABR thresholds minus ABR thresholds after electrode insertion) are shown in Figure 19-C. The organ of Corti ratings reflect a loss of hair cells in all experimental ears at the 25% (16kHz) location, in addition to supporting cell damage in some ears. At the 50% (4kHz) location, only subjects C77, C87 and C88 show significant hair cell loss. These assessments of hair cell loss are at least qualititatively related to measured hearing loss in that the greatest hearing loss is observed in ears C77, C87 and C88 with complete hair cell loss at both cochlear locations. Significant spiral ganglion cell depletion is evident in animals C84, C87 and C88.

These data demonstrate that we have achieved our goal of hair-cell damage corresponding to hearing loss in the basal turn. The spiral ganglion cell counts suggest that there is some neural degeneration, but both the histological and physiological data suggest that there are still significant numbers of surviving ganglion cells in the basal turn. Further analysis of more apical regions will be conducted to provide a complete base-to-apex assessment of cochlear and neural histopathology.

2.3.2 Physiological Results

For physiological recordings, intracochlear stimulation was provided by an 8-electrode, banded Nucleus-type electrode array with electrode numbering beginning at the tip (most apical) electrode. The array was inserted into the scala tympani. Dimensions of this array were scaled for the feline cochlea;

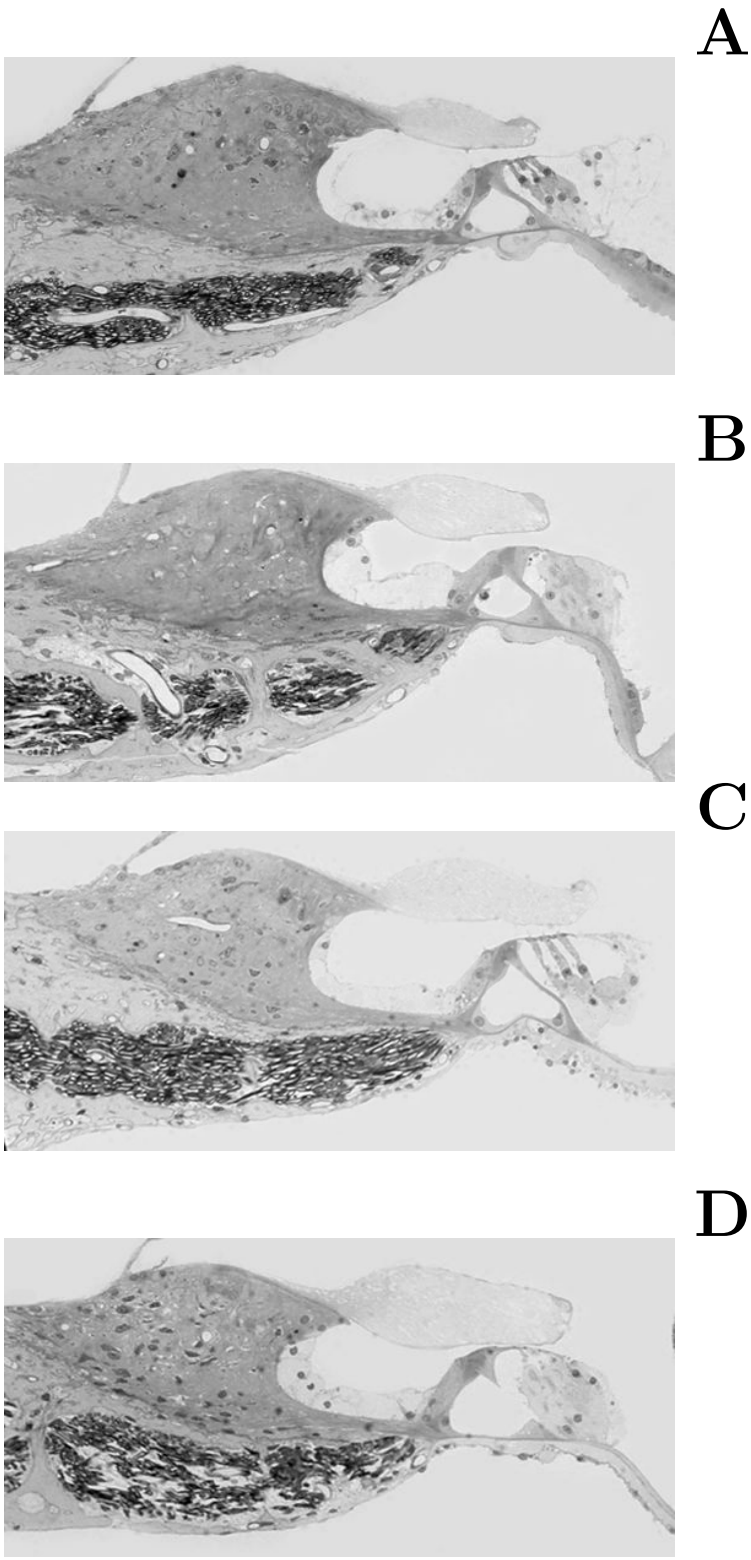

Figure 16: Sections through the organ of Corti and spiral lamina at 2 locations along the length of the cochlea comparing control to partially deafened animals: 25% (16 kHz) from the base, control (A) and deafened (B) and 50% (4 kHz) from the base, control (C) and deafened (D).

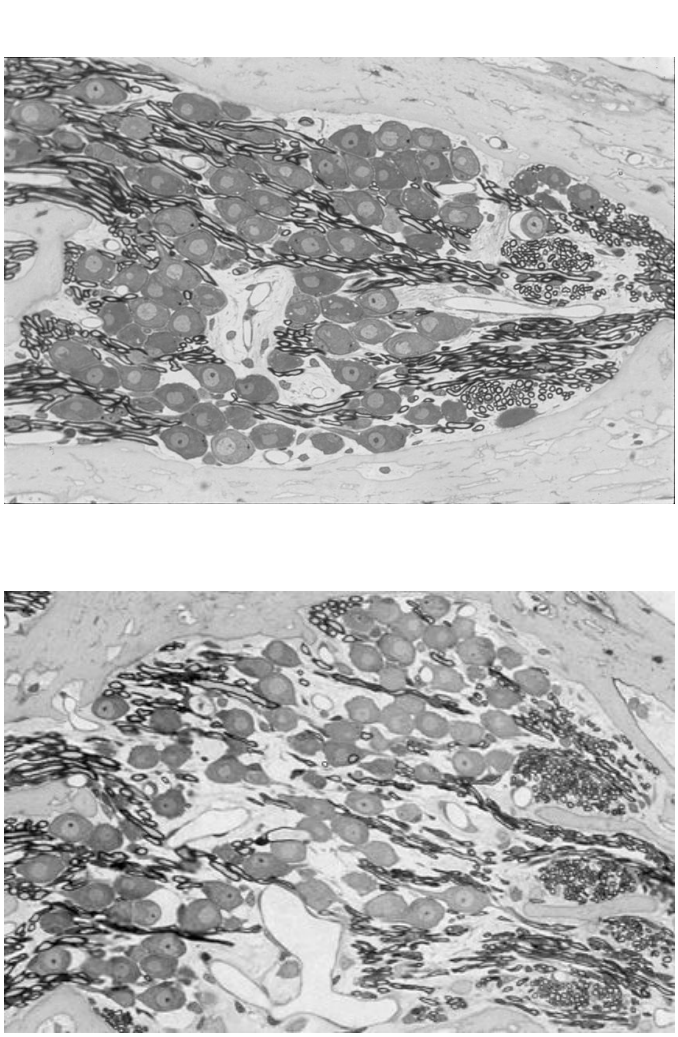

Figure 17: Sections throught Rosenthal's canal at a location 25% (16 kHz) of the length from the base, comparing a control animal (A) to a partially deafened animal (B).

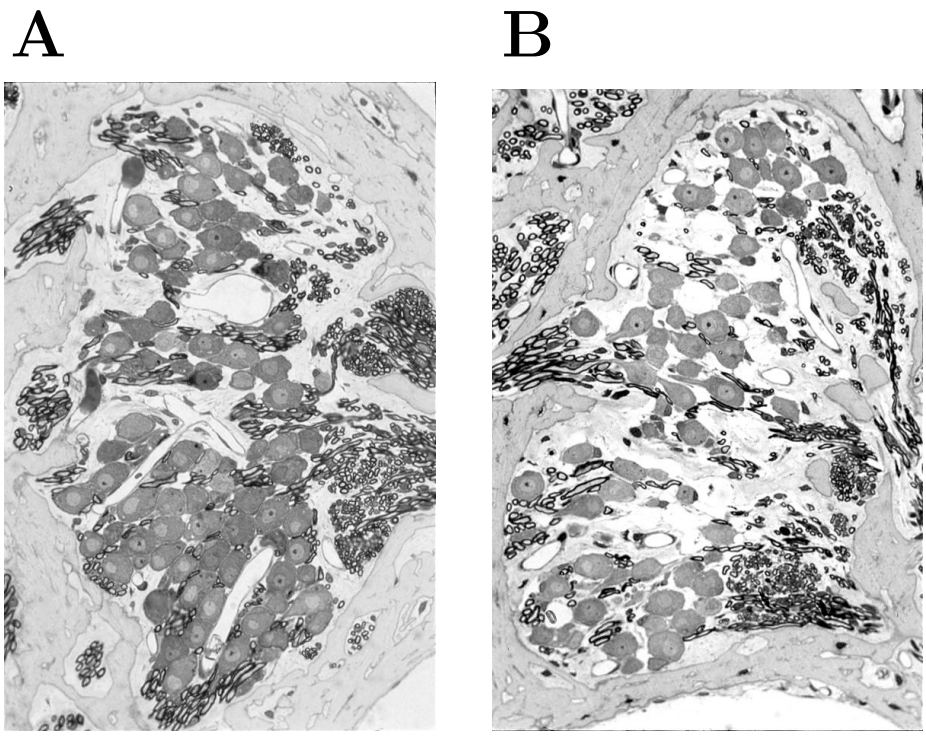

Figure 18: Sections through Rosenthal's canal at a location 50% (4 kHz) of the length from the base, comparing a control animal (A) to a partially deafened animal (B).

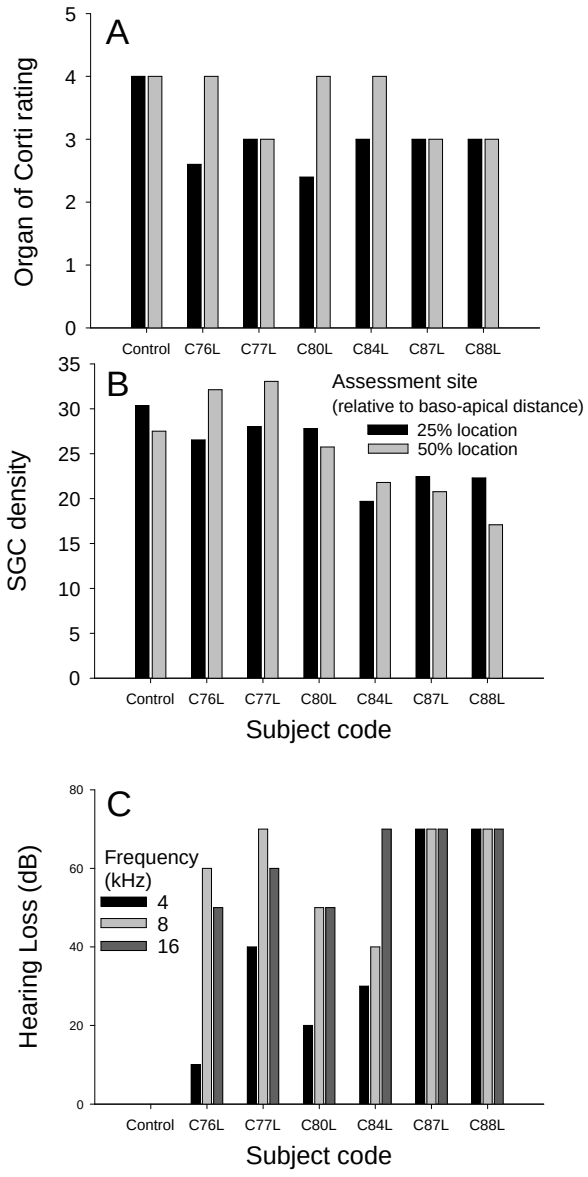

Figure 19: Results of histological analyses for six experimental ears and one control (untreated) ear. Organ of Corti rating, spiral ganglion cell density and hearing loss measures are defined in the text.

typically all 8 electrodes were inserted into the basal turn, past the plane of the round window. The use of this array enabled us to select different basal-to-apical sites of stimulation as well as to employ both monopolar and bipolar modes of current delivery. Prior to examining electric / acoustic stimulus interactions, detailed ECAP growth functions were measured for different electrode locations and configurations. Electric stimulation levels were then chosen on a per-subject basis for the acoustic masking study. In each case, we selected 6 to 8 levels spanning the dynamic range for the particular electrode configuration. ECAP responses were then obtained using a range of acoustic noise levels. In each case, the noise levels were chosen from those that showed little or no masking up to a maximum of 96 dB SPL overall level.

In Figure 20, ECAP growth functions are plotted for monopolar stimulation of the apical electrode in the array. Data are plotted for the six subjects in separate graphs. The average hearing loss ("Avg HL"), computed as the mean loss across 5 frequencies, is also indicated in each graph. In each case, the parameter is the acoustic noise level (in dB SPL overall level), indicated in each legend. Several trends are evident. First, there is generally a decrease in response amplitude in the presence of noise. We have observed no enhancement, or increase, in response amplitude in the presence of noise. This is consistent with previous observations in animals with more normal hearing (QPR 5). The decrease in response is most evident at high noise levels and the effect tends to be smaller (i.e., response amplitude increases) at lower noise levels. The effect is evident over a wide range of current levels, i.e., over a wide portion of the dynamic range. Finally, considered as a group, a trend may be evident that subjects with the most hearing loss display the least masking effects (Subjects C87 and C88). Those two subjects also had significant hair cell loss and spiral ganglion cell loss at the two locations evaluated histologically to date (cf. Figure 19).

In Figure 21, we present the acoustically masked ECAP data in another way to highlight the effect of the level of the acoustic noise. This figure presents ECAP amplitude as "average normalized amplitude". For this measure, we first computed, for each current level, the response amplitude with noise divided by the amplitude to the same electrical stimulus in quiet. These normalized amplitudes were then averaged across the 6-8 current levels (see Figure 3) and plotted as a function of acoustic noise level for each of the six subjects. With this manipulation, lower values on the ordinate scale correspond to greater degrees of masking. The parameter of each graph of

Figure 22 is the stimulus electrode configuration. Two monopolar configurations (Electrode 1 and 7) and one bipolar configuration (Electrode 1-2) were examined. Electrode 1 is the most apical in the array while Electrode 8 is the most basal. As noted for the data of Figure 21, there is a general trend where ECAP amplitude decreases with increasing noise level. The subjects with more residual hearing tend to show a decrease in response at lower stimulus levels (particularly C76, C80 and C84). Those subjects also showed no hair-cell pathology at the 50% (4 kHz) location of the cochlea (cf. Figure 20). Finally there is a clear trend that the apically located monopolar stimulating electrode produces the greatest masking effect while the bipolar configuration provides the least. These trends are all consistent with those expected in terms of overlap of the acoustic and electric responses with high-frequency hearing loss.

These data demonstrate that in subjects with high-frequency hearing loss and an electrode array implanted in the basal turn of the cochlea, there can still be significant interaction between electric and acoustic stimulation at the level of the auditory nerve. Those interactions tend to be greatest at high acoustic noise levels, but the interactions are evident at relatively low electric current levels as evidenced in Figure 20. The interactions tend to be less in subjects with greater hearing loss and more hair cell loss, although with six subjects and limited histological data available at this time, conclusions relative to significance cannot be made. Finally, with a relatively short electrode array (approximately 7 mm), there are clear variations in the interactions for stimulation of different electrode configurations, i.e. the most apical electrodes results in more interaction than the more basal electrode.

2.4 Binaural interaction

While most of our efforts focused on peripheral assessments of acoustic-electric interactions, we also investigated the possibility of acoustic-electric interactions manifested within the central nervous system, as per the mandate of the RFP. For this study, we employed a novel means of assessing the binaural ABR component that involves both electric and acoustic stimuli. Our initial goal was to determine the degree to which this novel measure could be used to assess central (brainstem) interactions. In doing so, we manipulated acoustic and electric stimulus parameters in an attempt to maximize any measurable interaction. Impulsive acoustic and electric stim-

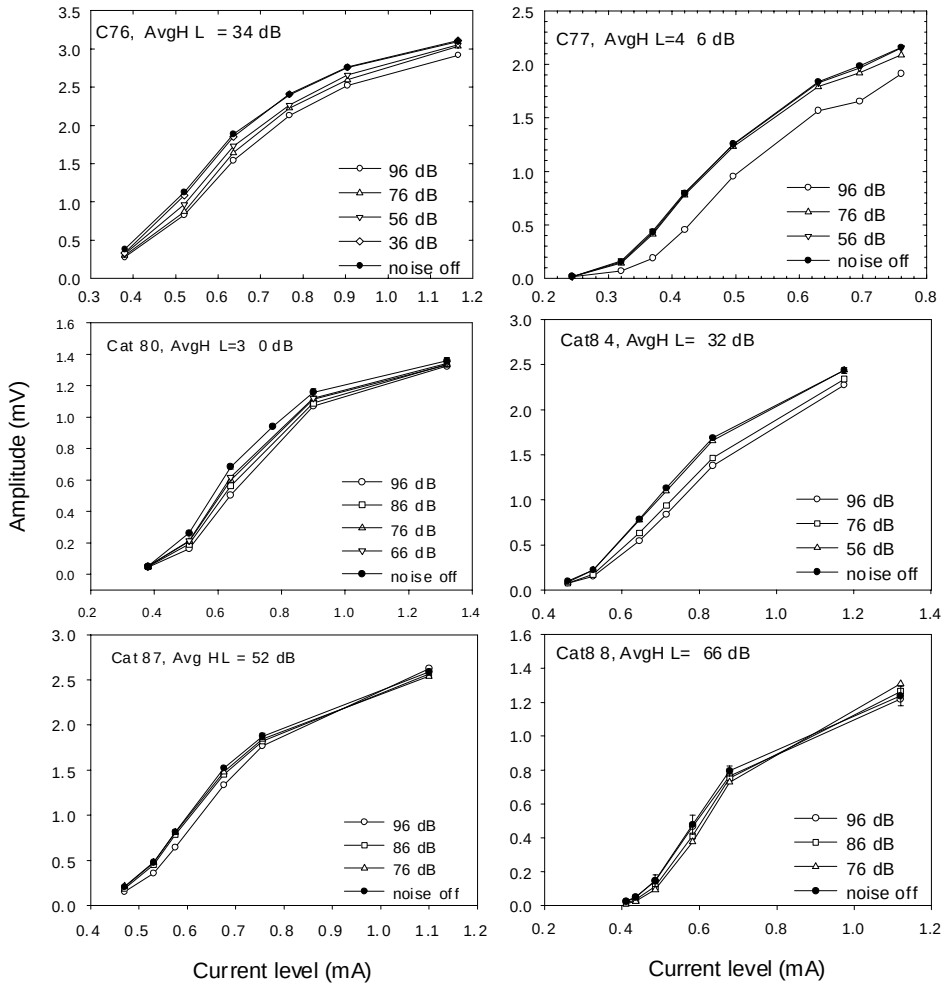

Figure 20: ECAP growth functions with and without a background of continuous white noise. Overall noise level in dB SPL is indicated in the legend.

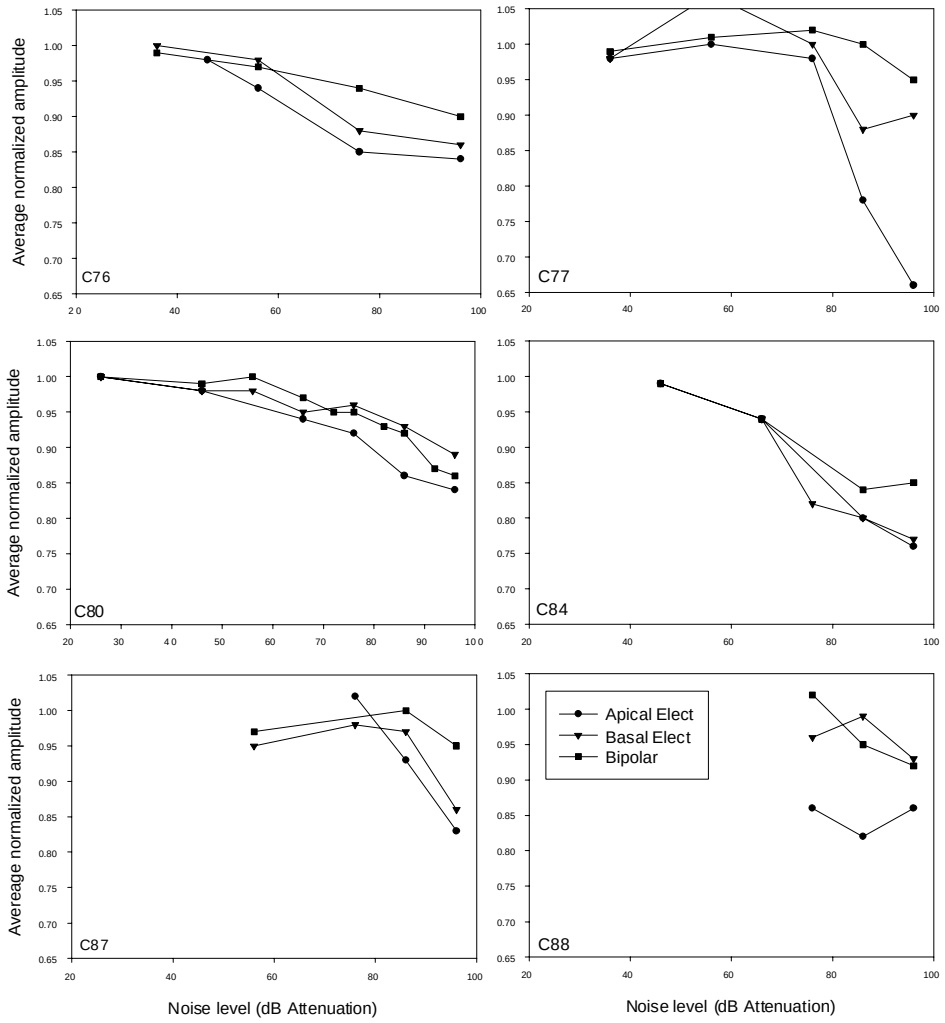

Figure 21: Average normalized amplitude is plotted as a function of noise level. Normalized amplitude is calculated as amplitude of the ECAP with noise divided by the amplitude of response in quiet. In each subject, the stimulus current levels were chosen to span the dynamic range. The average normalized amplitude is the average decrease across stimulus current levels. Values of 1 indicate no effect of noise. Values less than one indicate a decrease in the response in the presence of noise.

uli were employed in order to produce sufficient synchronous neural activity for robust ABR measures.

Guinea pigs were used in which hearing in the right ear was preserved while the left ear was deafened with local administration of neomycin. That ear was then implanted with an intracochlear electrode. The right ears received acoustic click stimuli, while the left cochleae received electric current pulses. Auditory brainstem responses to right-ear stimulation alone, left-ear stimulation alone, and stimulation of both ears were measured. To determine the binaural ABR component, the sum of responses to each ear alone was subtracted from the response to both ears. That derived response amplitude is plotted in Figure 22 as a function of time delay between electric and acoustic stimulation. The peak in binaural response tends to be between 1 and 1.5 ms, which is approximately the latency difference between acoustic and electric responses at the level of the auditory nerve. The amplitudes of these measures varied across subject and were generally small. Nevertheless, they show similar trends.

3 Summary

This final report summarizes the results from four sets of experiments designed to address issues related to effects of functional hair cells on the response to electrical stimulation of the auditory nerve.

- The first experiment set employed an animal model designed to maximize the effects of hair cells by minimizing hearing loss. Those results demonstrated significant changes in the direct neural response with functional hair cells.

- Those experiments were followed by a second set of experiments probing possible interactions between electric and acoustic stimulation in ears with functional hair cells. Those data demonstrated decreases in the response amplitude to electric stimulation in the presence of an acoustic stimulus. The results also demonstrated that those interactions can depend on the temporal aspects of acoustic-electric stimulation. For example, the relative phase of the two types of stimuli was an important variable. Also, acoustic and electric stimuli produced adaptation phenomena that were interactive. Finally, acoustic-electric interactions were shown to be dependent on the spectral characteristics

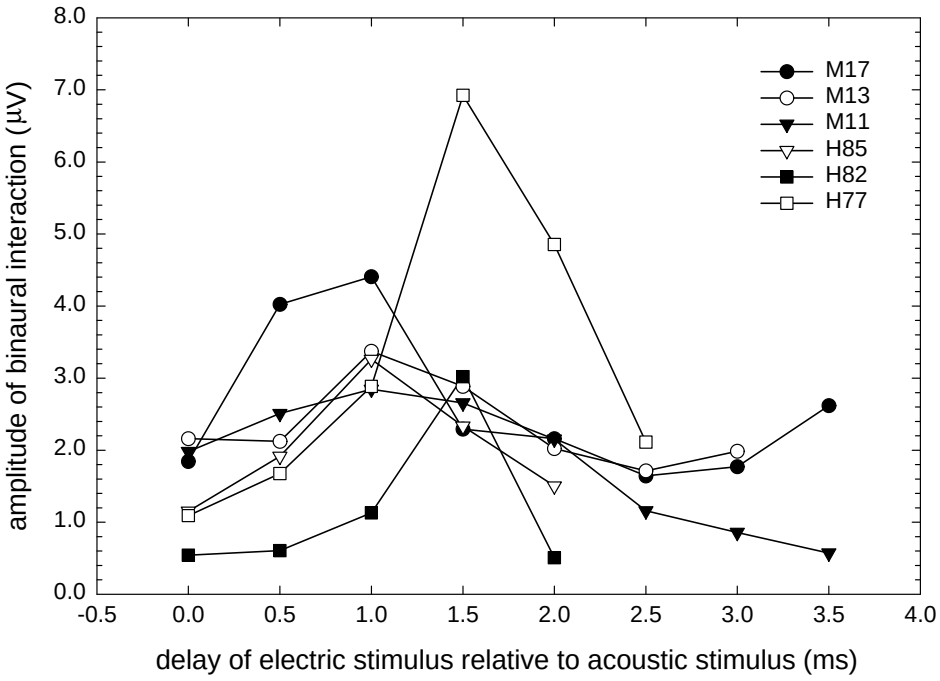

Figure 22: Effect of presentation of acoustic stimulus in one ear and electric stimulus in the contralateral ear. Plotted is the amplitude of the binaural ABR component as a function of delay between acoustic click (presented to right ear) and electric biphasic pulse (presented to the left ear). Data from 6 guinea pigs are shown. The binaural interaction component produces a peak when the electric stimulus is delayed (relative to the acoustic stimulus) by 1 to 1.5 ms.

of the acoustic stimulus.

- Based on the aforementioned spectral interactions, a third set of experiments investigated the acoustic-electric interactions in animals with hearing loss, attempting to simulate that typical of a prospective cochlear implant user. Those data also demonstrated the potential for acoustic-electric interactions in that population.
- Finally, the results from the fourth set of experiments suggested that, if there is significant residual hearing in the opposite ear, there can be significant binaural interaction between acoustic and electric stimulation

Individuals with significant hearing who have received a cochlear implant generally have relatively good low-frequency hearing, poor high-frequency hearing and the implant is limited to the basal portion of the cochlea. In this way, acoustic stimulation may primarily stimulate apical neurons while electrical stimulation may be primarily confined to basal fibers. However, spatial spread of electrical stimulation can result in overlap of acoustically and electrically stimulated neurons. These results suggest that in such ears there may significant interaction between acoustic and electric stimulation. Furthermore, in some cases, such as those showing an increase in stochastic response properties, stimulating neurons with functional hair cells may result in improved signal transmission (increased dynamic range, less response alternation) to the central nervous system.

References

[1] Brummett R.E., Brown R.T., Hines D.L. (1979). Quantitative relationships of the ototoxic interaction of kanamycin and ethacrynic acid. Arch Otolaryngol., 105, 240-246.

[2] Dobie R.A., Berlin C.I. (1979). Binaural interaction in brainstem-evoked responses. Arch Otolaryngol., 105, 391-398.

[3] Kiang N.Y.S., Liberman M.C., Levine R.A. (1976). Auditory nerve activity in cat exposed to ototoxic drugs and high-intensity sounds. Ann. Otol. Rhinol. Laryngol., 85, 752-768.

[4] Leake P.A., Hradek G.T. (1988). Cochlear pathology of long term neomycin induced deafness in cats. Hear. Res., 33, 11-34.

[5] Leake P.A., Hradek G.T., Rebscher S.J., Snyder R.L. (1991). Chronic intracochlear electrical stimulation induces selective survival of spiral ganglion neurons in neonatally deafened cats. Hear. Res., 54, 251-271.

[6] Leake-Jones P.A., Vivion M.C., O'Reilly B.F., Merzenich M.M. (1982). Deaf animal models for studies of a multichannel cochlear prosthesis. Hear. Res., 8, 225-246.

[7] Liberman M.C. (1982) The cochlear frequency map for the cat: labeling auditory-nerve fibers of known characteristic frequency. J. Acoust. Soc. Am. 72, 1441-1449.

[8] Matsuoka A.J., Abbas P.J., Rubinstein J.T., Miller C.A. (2000) The neuronal response to electrical constant-amplitude pulse train stimulation: evoked compound action potential recordings. Hear. Res. 149, 115-128.

[9] Miller C.A., Abbas P.J., Robinson B.K. (1994). The use of long-duration current pulses to assess nerve survival. Hear. Res., 78, 11-26.

[10] Miller C.A., Abbas P.J., Rubinstein J.T., Robinson B.K., Matsuoka A.J., Woodworth, G. (1998) Electrically evoked compound action potentials of guinea pig and cat: response to monopolar, monophasic stimulation. Hear. Res., 119, 142-154.

[11] Miller C.A., Abbas P.J., Rubinstein J.T., Robinson B.K., & Matsuoka A.J. (1999a). Electrically evoked single-fiber Action potentials from cat: responses to monopolar, monophasic stimulation. Hear. Res., 130, 197-218.

[12] Miller C.A., Abbas, P.J., Rubinstein J.T. (1999b) An empirically based model of the electrically evoked compound action potential. Hear. Res. 135, 1-18.

[13] Moxon E.C. (1971). Neural and mechanical responses to electrical stimulation of the cat's inner ear. Doctoral Dissertation, MIT, Cambridge, MA.

[14] Russell N.J., Fox K.E., Brummett R.E. (1979) Ototoxic effects of the interaction between kanamycin and ethacrynic acid. Acta Otolaryngol. 88, 369-381.

[15] Shepherd R.K., Clark G.M., Black R.C. (1983) Chronic electrical stimulation of the auditory nerve. Physiological and histopathological results. Acta Otolaryngol (Stockh) Suppl. 339, 19-31.

[16] Spoendlin H. (1975). Retrograde degeneration of the cochlear nerve. Acta Otolaryngol., 79, 266-275.

[17] Spoendlin H., Brun J.P. (1974). The block-surface technique for evaluation of cochlear pathology. Arch. Otol. Rhinol. Laryngol., 208, 137-145.

[18] Spurr A.R. (1969). A low-viscosity epoxy resin embedding medium for electron microscopy. Ultrastructure Res., 26, 31.

[19] van den Honert C., Stypulkowski P.H. (1984). Physiological properties of the electrically stimulated auditory nerve. II. Single fiber recordings. Hear. Res., 14, 225-243.

[20] Weibel E.R. (1979). Stereological methods: Vol. 1 - Practical methods for biological morphometry. NewYork: Academic Press.

[21] West B.A., Brummett R.E., Himes D.L. (1973). Interaction of kanamycin and ethacrynic acid. Arch. Otolaryngol. 98, 32-37.

[22] Wilson B.S., Finley C.C., Zerbi M., Lawson D.T. (1994) Seventh Quarterly Progress Report. NIH Contract N01-DC-2-2401.

[23] Xu J., Shepherd R.K., Millard R.E., Clark G.M. (1993). Chronic electrical stimulation of the auditory nerve at high stimulus rates: a physiological and histopathological study. Hear. Res., 105, 1-29.

[24] Young E.D. Sachs, M.B. (1973). Recovery of detection probability following sound exposure: Comparison of physiology and psychophysics. J. Acoust. Soc. Am., 87, 1544-1553.